PHYSICAL REVIEW D **74,** 075008 (2006)

Resonances from two universal extra dimensions

Gustavo Burdman,[1] Bogdan A. Dobrescu,[2] and Eduardo Pontón[3]

[1]*Instituto de Física, Universidade de São Paulo, São Paulo, SP 05508-900, Brazil*

[2]*Fermilab, Batavia, Illinois 60510, USA*

[3]*Department of Physics, Columbia University, New York, New York 10027, USA*

(Received 3 August 2006; published 20 October 2006)

Standard model gauge bosons propagating in two universal extra dimensions give rise to heavy spin-1 and spin-0 particles. The lightest of these, carrying Kaluza-Klein numbers (1,0), may be produced only in pairs at colliders, whereas the (1,1) modes, which are heavier by a factor of $\sqrt{2}$, may be singly produced. We show that the cascade decays of (1,1) particles generate a series of closely-spaced narrow resonances in the $t\bar{t}$ invariant mass distribution. At the Tevatron, s-channel production of (1,1) gluons and electroweak bosons will be sensitive to $t\bar{t}$ resonances up to masses in the 0.5–0.7 TeV range. Searches at the LHC for resonances originating from several higher-level modes will further test the existence of two universal extra dimensions.

DOI: 10.1103/PhysRevD.74.075008 PACS numbers: 12.60.−i, 11.25.Mj, 14.80.−j

I. INTRODUCTION

If the standard model gauge bosons propagate in extra dimensions, then for each of the $SU(3)_C \times SU(2)_W \times U(1)_Y$ gauge fields there is a tower of heavy vector bosons that could produce signals in collider experiments. These heavy vector bosons are commonly called Kaluza-Klein (KK) modes of the gauge bosons [1], and we will refer to them in what follows as ''vector modes.'' The properties of the vector modes depend crucially on the number, compactification and metric of extra dimensions, as well as on what other fields propagate in the extra dimensions.

For example, if the metric is flat and no quarks or leptons propagate in the extra dimensions, then vector-mode exchange among fermions produces too large corrections to the electroweak observables, unless the compactification scale (which approximately sets the mass of the lightest vector modes within each tower, called level-1 states) is higher than roughly 6 TeV [2], pushing the vector modes beyond the reach of the Large Hadron Collider (LHC) [3]. By contrast, if the extra dimensions are universal, i.e., all standard model particles propagate in the extra dimensions, then the limit on the compactification scale is close to the electroweak scale [4], so that the vector modes could be produced not only at the LHC but also at the Tevatron. In that case, however, a KK parity is conserved implying that level-1 vector modes may be produced only in pairs, and that their decays involve soft leptons and jets plus missing energy [5], making their discovery challenging.

The vector modes that are particularly interesting for collider searches are level-2 states from universal extra dimensions. These have individual couplings to the observed fermions, induced by loops within the higher-dimensional effective theory [6], or by boundary operators generated at the cutoff scale, M_s, where some new physics should smooth out the ultraviolet behavior of the theory [4]. The induced couplings are rather small, being suppressed by either a loop factor or a volume factor, so that one need not worry about the constraints from electroweak precision measurements. At the same time, the suppression may be not too strong, allowing a potentially sizable s-channel production at high-energy colliders. This possibility in the case of one universal extra dimension, where the level-2 masses are roughly twice as large as the level-1 masses, has been noted in Ref. [5] and analyzed in detail in Ref. [7].

In this paper we point out that level-2 vector modes in the case of *two* universal extra dimensions offer better opportunities for discovery. The reason is that the level-2 vector modes in this case have masses which are larger than the level-1 masses by a factor of approximately $\sqrt{2}$. As a result, their production is possible at smaller center-of-mass energies, and the decays of level-2 states into pairs of level-1 states, which would lead to only soft leptons and jets in the detector, are kinematically forbidden (as opposed to the case of one universal extra dimension where such decays are typically allowed). Then the level-2 states, characterized by KK numbers (1,1), have large branching fractions for decays into a pair of standard model particles giving rise to a high p_T signal. Another distinctive feature of two universal extra dimensions is that each vector mode is accompanied by a spin-0 particle in the adjoint representation of the corresponding gauge group.

In Sec. II we present the standard model in two universal extra dimensions compactified on the chiral square, which is the simplest compactification consistent with the chirality of the quarks and leptons. We concentrate especially on the mass spectrum and KK-number-violating interactions of the KK modes. In Sec. III we compute in detail the branching fractions of the (1,1) modes, which is useful for any future phenomenological study of the standard model in six dimensions. We then turn to resonant production of the (1,1) modes at the Tevatron, and estimate the expected reach of Run II in Sec. IV. The more complex phenomenology at the LHC is briefly discussed in Sec. V, and then our results are summarized in Sec. VI.

II. SIX-DIMENSIONAL STANDARD MODEL

We consider the standard model in six dimensions, with two dimensions compactified. Each of the gauge fields has six components: for example, the six-dimensional (6D) gluon field G^a_α, where a labels the eight $SU(3)_C$ generators, has a 6D Lorentz index $\alpha = 0, 1, \ldots, 5$. The quark and lepton fields are chiral 6D fermions, which have four components. The requirements of 6D anomaly cancellations and fermion mass generation [8] force the weak-doublet quarks to have opposite 6D chirality than the weak-singlet quarks, so that the quarks of one generation are given by $Q_+ = (U_+, D_+)$, U_-, D_-, where $\pm$ labels the 6D chiralities. The chirality assignment in the 6D lepton sector is similar (its implications for the neutrino masses are analyzed in [9]).

The zero-mode states, which are particles of zero momentum along the extra dimensions, are identified with the observed standard model particles. Since the observed quarks and leptons have definite 4D chirality, an immediate constraint on any 6D extension of the standard model is that the compactification of the two extra dimensions must allow chiral zero-mode fermions. A simple compactification of this type has been studied in detail in [10,11]. It consists of a square, $0 \leq x_4, x_5 \leq \pi R$, where x_4, x_5 are the coordinates of the extra dimensions and R is the compactification "radius." The compactification is obtained by imposing the identification of two pairs of adjacent sides of the square, and we refer to it as the "chiral square."

A. KK decomposition

For any 6D field $\Phi(x^\mu, x^4, x^5)$ that has a zero mode, the field equations have the following solution:

$$\Phi = \sum_{j,k} \left(\cos\frac{jx^4 + kx^5}{R} + \cos\frac{kx^4 - jx^5}{R} \right) \frac{\Phi^{(j,k)}(x^\mu)}{\pi R(1 + \delta_{j,0})}. \tag{2.1}$$

The KK numbers, j and k, are integers with $j \geq 1$ and $k \geq 0$, or $j = k = 0$. The 4D fields $\Phi^{(j,k)}(x^\mu)$ are the KK modes of the 6D field Φ. They have masses due to the momentum along x^4, x^5 given by

$$M_{j,k} = \frac{1}{R}\sqrt{j^2 + k^2}, \tag{2.2}$$

so that the mass spectrum, in the limit where other contributions to physical masses are neglected, starts with $M_{0,0} = 0$, $M_{1,0} = 1/R$, $M_{1,1} = \sqrt{2}/R$, $M_{2,0} = 2/R, \ldots$ For 6D fields that do not have a zero mode, the KK decompositions differ from Eq. (2.1), as shown in [10,11], but their KK mass spectrum is the same for the massive states.

The 6D gluon and electroweak gauge bosons decompose each into a tower of 4D spin-1 fields, a tower of 4D spin-0 fields which are eaten by the heavy spin-1 fields, and a tower of 4D spin-0 fields which remain in the spectrum, all belonging to the adjoint representation of the corresponding gauge group. We refer to these latter spin-0 fields as "spinless adjoints." The zero modes of the spin-1 fields are the standard model gauge bosons, while the spin-0 fields do not have zero modes. Therefore, in the unitary gauge the 6D gluon field includes at each nonzero KK level a vector mode $G^{(j,k)a}_\mu$ and a real scalar field $G^{(j,k)a}_H$. The 6D weak gauge fields have KK modes $W^{(j,k)\pm}_\mu$, $W^{(j,k)\pm}_H$, $W^{(j,k)3}_\mu$, and $W^{(j,k)3}_H$, while the hypercharge KK gauge bosons are $B^{(j,k)}_\mu$, $B^{(j,k)}_H$. Electroweak symmetry breaking due to the 6D VEV of the Higgs doublet (as discussed in general in [11]), mixes $W^{(j,k)3}_\mu$ and $B^{(j,k)}_\mu$, as well as $W^{(j,k)3}_H$ and $B^{(j,k)}_H$. However, for $1/R \gtrsim 300$ GeV, this mixing is small [6], and we will neglect it in what follows. The 6D Higgs doublet decomposes into a tower of 4D weak doublets. The zero-mode doublet gives the longitudinal degrees of freedom of the W and Z and a Higgs boson, while at each nonzero KK level three of the degrees of freedom of the massive Higgs doublet mix with the longitudinal components of the electroweak vector modes (this mixing is also suppressed by $M_Z R$).

The 6D quark and lepton fields decompose each into a tower of heavy vectorlike 4D fermions and a chiral zero mode identified with the observed fermion. Explicitly, the standard model quark doublets are given by $(u_L, d_L) \equiv Q^{(0,0)}_{+_L}$, while the standard weak-singlet quarks are $u_R \equiv U^{(0,0)}_{-_R}$ and $d_R \equiv D^{(0,0)}_{-_R}$, where a generation index is implicit.

B. Localized operators

The "chiral square" compactification is a two-dimensional space having the topology of a sphere. It is flat everywhere, with the exception of conical singularities at the corners of the square. Altogether there are three such conical singularities, given that the $(0, \pi R)$ and $(\pi R, 0)$ corners are identified.

Operators localized at the singular points are generated by loops involving the bulk interactions [12], as in the theories studied in Ref. [6,13]. The space around the conical singularities is symmetric under rotations in the (x^4, x^5) plane, and therefore the localized operators have an $SO(2)$ symmetry. Furthermore, the bulk interactions are symmetric under reflections with respect to the center of the square. This symmetry is a KK parity, labeled by Z_2^{KK}. It implies that the operators generated at (0,0) are identical with those at $(\pi R, \pi R)$.

Other contributions to the localized operators might be induced by physics above the cutoff scale. They should also be $SO(2)$ symmetric. In addition, it is compelling to assume that these UV-generated localized operators are Z_2^{KK} symmetric, so that the stability of the lightest KK particle, a promising dark matter candidate [14], is ensured.

The 4D Lagrangian can be written as

$$\int_0^{\pi R} dx^4 \int_0^{\pi R} dx^5 \{\mathcal{L}_{\rm bulk} + \delta(x_4)\delta(\pi R - x_5)\mathcal{L}_2 + [\delta(x_4)\delta(x_5) + \delta(\pi R - x_4)\delta(\pi R - x_5)]\mathcal{L}_1\}. \quad (2.3)$$

$\mathcal{L}_{\rm bulk}$ includes 6D kinetic terms for the quarks, leptons, $SU(3)_C \times SU(2)_W \times U(1)_Y$ gauge fields, and a Higgs doublet, 6D Yukawa couplings of the quarks and leptons to the Higgs doublet, and a 6D Higgs potential. The form of these terms can be derived from the general 6D Lagrangians discussed in [10,11]. $\mathcal{L}_1$ and $\mathcal{L}_2$ contain all the localized operators. In particular, these include 4D-like kinetic terms for all 6D fields, and the pieces of 6D kinetic terms that describe motion along the extra dimensions. For example, the localized operators of the lowest mass dimension that involve the 6D quark field U_- appear in $\mathcal{L}_p$ $(p = 1, 2)$ as

$$\frac{C_{pU}}{2^2 M_s^2} i\bar{U}_{-_R}\Gamma^\mu D_\mu U_{-_R} + \left(\frac{C'_{pU}}{2^2 M_s^2} i\bar{U}_{-_R}\Gamma^l D_l U_{-_L} + \text{H.c.}\right), \quad (2.4)$$

where Γ^μ with $\mu = 0, 1, 2, 3$ and Γ^l with $l = 4, 5$ are anticommuting 8×8 matrices, D_μ, D_l are covariant derivatives, C_{pU} (C'_{pU}) are real (complex) dimensionless parameters, and M_s is the cutoff scale. For convenience, we also wrote explicit factors of $(1/2)^2$ to account for an enhancement due to the values of the wave functions in Eq. (2.1) at the singular points. The localized operators of the lowest mass dimension that involve the 6D gluon field are given by

$$\mathcal{L}_p \supset -\frac{1}{4}\frac{C_{pG}}{2^2 M_s^2} G^{\mu\nu} G_{\mu\nu} - \frac{1}{2}\frac{C'_{pG}}{2^2 M_s^2}(G_{45})^2, \quad (2.5)$$

where C_{pG} and C'_{pG} with $p = 1, 2$ are real dimensionless parameters.

As mentioned above, the contributions to the localized operators in Eq. (2.4) and (2.5) arise from two sources: loops with KK modes, and physics above the cutoff scale. The bare contribution, from physics at or above the cutoff scale, to the coefficients of the localized terms can be estimated by assuming that the localized couplings get strong at the cutoff scale M_s, where M_s is the scale at which the QCD interactions become strong in the ultraviolet. Using naive dimensional analysis (NDA) in the 6D theory [15], we estimate the coefficients C_{pG} and C'_{pG} in Eq. (2.5), C_{pU}, $\text{Re}C'_{pU}$, $\text{Im}C'_{pU}$ in Eq. (2.4), and the analogous coefficients associated with the Q_+ and D_- fields, to be all of the order of $l_6/l_4 = 8\pi$, where $l_6 = 128\pi^3$ and $l_4 = 16\pi^2$ are 6D and 4D loop factors, respectively. This estimate assumes that the localized term receives contributions from color interactions. If this is not the case, then there is an associated suppression.

Furthermore, NDA gives $(\pi R M_s)^2 \sim l_6/(g_s^2 N_c)$, where g_s is the 4D QCD gauge coupling and $N_c = 3$ is the number of colors. Thus, the bare contribution to the effective 4D coupling is of the order of $(l_6/l_4)/(\pi R M_s)^2 \sim g_s^2 N_c/l_4$. Also, the separation between the compactification scale and the cutoff scale is

$$M_s R \sim \left(\frac{32}{\alpha_s N_c}\right)^{1/2} \approx 10. \quad (2.6)$$

The strong coupling constant is evaluated here at the compactification scale, $1/R$: $\alpha_s \equiv g_s^2/(4\pi) \approx 0.1$.

The localized operators are also renormalized by the physics below the cutoff scale, M_s. These contributions were calculated in [12] at one-loop order. For the fermion kinetic terms in Eq. (2.4) involving 4D derivatives, one obtains

$$\frac{C_{1f}}{(\pi M_s R)^2} = \left[-4\sum_A g_A^2 C_2(f) + \frac{5}{8}\sum_i \lambda_i^2\right]\frac{1}{16\pi^2}\ln\frac{M_s^2}{\mu^2},$$
$$\frac{C_{2f}}{(\pi M_s R)^2} = \left[-2\sum_A g_A^2 C_2(f) + \frac{1}{4}\sum_i \lambda_i^2\right]\frac{1}{16\pi^2}\ln\frac{M_s^2}{\mu^2}, \quad (2.7)$$

where λ_i are Yukawa couplings of the fermion f to *complex* scalars having zero modes (the i sum is over the scalars), g_A is the 4D gauge coupling, $C_2(A)$ and $C_2(f)$ are the quadratic Casimir eigenvalues of the gauge fields and fermions, respectively [for an $SU(N)$ gauge group, $C_2(A) = N$, and if f is in the fundamental representation, $C_2(f) = (N^2 - 1)/(2N)$], and $T(f)$ and $T(s)$ are the indices of the representations to which the fermion f and scalar s belong [$T(f) = T(s) = 1/2$ in the fundamental representation]. Notice that these contributions are scale dependent, and μ should be taken of the order of the characteristic scale of the process of interest.

For the coefficients of the fermion kinetic terms with derivatives in the plane of the extra dimensions, one finds that only the Yukawa couplings contribute:

$$\frac{C'_{1f}}{(\pi M_s R)^2} = \frac{5}{8}\sum_i \lambda_i^2 \frac{1}{16\pi^2}\ln\frac{M_s^2}{\mu^2},$$
$$\frac{C'_{2f}}{(\pi M_s R)^2} = \frac{1}{4}\sum_i \lambda_i^2 \frac{1}{16\pi^2}\ln\frac{M_s^2}{\mu^2}, \quad (2.8)$$

where again the sum runs over complex scalars.

The coefficients of the 4D gauge kinetic terms in Eq. (2.5) are found to be

$$\frac{C_{1A}}{(\pi M_s R)^2} = \left[-\frac{14}{3}C_2(A) + \frac{2}{3}\sum_f T(f) + \frac{5}{12}\sum_s T(s)\right]\frac{g_A^2}{16\pi^2} \times \ln\frac{M_s^2}{\mu^2}, \quad (2.9)$$
$$\frac{C_{2A}}{(\pi M_s R)^2} = \left[-2C_2(A) + \frac{1}{6}\sum_s T(s)\right]\frac{g_A^2}{16\pi^2}\ln\frac{M_s^2}{\mu^2},$$

where A stands for any gauge field. The sum over f involves all 6D Weyl fermions having a zero mode of

any 4D chirality, while the sum over s involves all complex scalars having a zero mode.

Finally, for the operators involving the spinless adjoints A_4–A_5 one finds

$$\frac{C'_{1A}}{(\pi M_s R)^2} = \left[8C_2(A) - 4\sum_f T(f) + \frac{13}{4}\sum_s T(s) \right] \frac{g_A^2}{16\pi^2} \times \ln\frac{M_s^2}{\mu^2}, \tag{2.10}$$

$$\frac{C'_{2A}}{(\pi M_s R)^2} = \left[2C_2(A) + \frac{1}{2}\sum_s T(s) \right] \frac{g_A^2}{16\pi^2} \ln\frac{M_s^2}{\mu^2},$$

where again the sums run over 6D Weyl fermions and complex scalars having zero modes.

We note that the contribution due to the physics below the cutoff scale is enhanced by a logarithmic factor compared to the ''bare'' contributions from physics at or above M_s. However, in the present class of models the logarithm is at most a few [see Eq. (2.6)]. Also, for strongly interacting particles one should worry about higher-loop orders in the contributions to the localized operators coming from the physics below M_s. For these strongly interacting particles, the multiloop effects are of the same order as the one-loop result. Note, however, that for particles that do not interact directly with colored states, such as the leptons, the one-loop computation should be a good approximation for the coefficient of the localized operator, modulo the bare contributions which are not logarithmically enhanced. At any rate, the above results should be used carefully and we shall take them as an estimate of the physics due to localized operators. For the most part, we will express our results in terms of generic localized parameters. However, for numerical purposes we will use the above one-loop expressions.

C. Mass spectrum

The localized terms of Eqs. (2.4) and (2.5) shift the masses of the fermion, gauge field and spinless adjoint KK modes, leading to mass splittings among the members of a given KK level. To lowest order in the localized terms C_{pf}, C'_{pf}, C_{pA}, and C'_{pA}, where f stands for any of the fermions and A for any of the gauge fields, the mass shifts are

$$\begin{aligned} M_{f^{(j,k)}} &= M_{j,k}\left(1 - \frac{1}{2}\delta Z_{f^{(j,k)}} + \frac{1}{2}\delta Z'_{f^{(j,k)}}\right), \\ M_{A^{(j,k)}} &= M_{j,k}\left(1 - \frac{1}{2}\delta Z_{A^{(j,k)}}\right), \\ M_{A_H^{(j,k)}} &= M_{j,k}\left(1 + \frac{1}{2}\delta Z_{A_H^{(j,k)}}\right). \end{aligned} \tag{2.11}$$

For KK-parity even fields, that is (j,k) modes with $(-1)^{j+k} = +1$, we find

$$\begin{aligned} \delta Z_{f^{(j,k)}} &= \frac{1}{(\pi M_s R)^2}(2C_{2f} + C_{2f}), \\ \delta Z'_{f^{(j,k)}} &= \frac{2}{(\pi M_s R)^2}\,\mathrm{Re}(2C'_{1f} + C'_{2f}), \\ \delta Z_{A^{(j,k)}} &= \frac{1}{(\pi M_s R)^2}(2C_{1A} + C_{2A}), \\ \delta Z_{A_H^{(j,k)}} &= \frac{1}{(\pi M_s R)^2}(2C'_{1A} + C'_{2A}), \end{aligned} \tag{2.12}$$

while for KK-parity odd fields, i.e., $(-1)^{j+k} = -1$, the δZ's are given by (2.12) with $C_{2f} = C'_{2f} = C_{2A} = C'_{2A} = 0$. The mass shifts depend on the quantum numbers j and k because the coefficients C_{pf}, C'_{pf}, C_{pA} and C'_{pA} are running parameters and should be evaluated at the scale of the corresponding mass $M_{j,k}$.

The mass of the gluon vector mode, $G_\mu^{(j,k)}$, can be parametrized as

$$M_{G^{(j,k)}} = M_{j,k}(1 + A_G C_{j,k}^G), \tag{2.13}$$

where

$$C_{j,k}^G \equiv \frac{g_s^2 N_c}{16\pi^2} \ln\left(\frac{M_s^2}{M_{j,k}^2}\right), \tag{2.14}$$

$M_{j,k}$ are the masses due to motion in the extra dimensions, given in Eq. (2.2), and A_G is a dimensionless parameter expected to be of order unity. The $SU(2)_W$-doublet quark modes have masses

$$M_{Q_+^{(j,k)}} = M_{j,k}\left(1 + A_{Q_+} C_{j,k}^G + \frac{m_q^2}{2M_{j,k}^2}\right), \tag{2.15}$$

where m_q is the mass of the zero-mode quark, and we expanded in $m_q^2/M_{j,k}^2 \ll 1$. We employ a similar parametrization for the $SU(2)_W$-singlet quarks in terms of dimensionless parameters, A_{U_-} and A_{D_-} (collectively denoted by A_{Q_-}). The coefficients A_{Q_+}, A_{U_-} and A_{D_-} are also expected to be of order unity.

The masses of the hypercharge and electrically-neutral $SU(2)_W$ vector modes, $B_\mu^{(j,k)}$ and $W_\mu^{(j,k)3}$, are given by

$$\begin{aligned} M_{W^{(j,k)}} &= M_{j,k}\left(1 + \frac{2g^2}{N_c g_s^2} A_W C_{j,k}^G + \frac{M_W^2}{2M_{j,k}^2}\right), \\ M_{B^{(j,k)}} &= M_{j,k}\left(1 + \frac{g'^2}{N_c g_s^2} A_B C_{j,k}^G\right), \end{aligned} \tag{2.16}$$

where g and g' are the 4D $SU(2)_W$ and $U(1)_Y$ gauge couplings, respectively. In Eqs. (2.16), we have neglected terms of order $(M_W/M_{j,k})^4$, where M_W is the zero-mode W mass. Similar parametrizations can be used for the masses of the spinless adjoints:

$$M_{G_H^{(j,k)}} = M_{j,k}(1 + A_{G_H} C^G_{j,k}),$$
$$M_{W_H^{(j,k)}} = M_{j,k}\left(1 + \frac{2g^2}{N_c g_s^2} A_{W_H} C^G_{j,k} + \frac{M_W^2}{2M_{j,k}^2}\right), \qquad (2.17)$$
$$M_{B_H^{(j,k)}} = M_{j,k}\left(1 + \frac{g'^2}{N_c g_s^2} A_{B_H} C^G_{j,k}\right).$$

The $SU(2)_W$-doublet and -singlet lepton modes, $L^{(j,k)}$ and $E^{(j,k)}$, have masses

$$M_{L^{(j,k)}} = M_{j,k}\left(1 + \frac{2g^2}{N_c g_s^2} A_L C^G_{j,k}\right),$$
$$M_{E^{(j,k)}} = M_{j,k}\left(1 + \frac{g'^2}{N_c g_s^2} A_E C^G_{j,k}\right). \qquad (2.18)$$

The above corrections to the KK masses of leptons and electroweak bosons are due to the 6D $SU(2)_W \times U(1)_Y$ interactions. Given that the loop factor $C^G_{j,k}$ is computed for QCD, we have factored out the electroweak gauge couplings such that the coefficients $A_W, A_B, A_{W_H}, A_{B_H}, A_L$, and A_E are all expected to be of order unity, barring enhancement factors due to particle multiplicities.

The KK modes of the Higgs boson, $h^{(j,k)}$, are split in mass from the KK modes of the other 3 degrees of freedom of the Higgs doublet. The latter ones mix with the $W_H^{(j,k)}$ KK modes, giving rise to the Nambu-Goldstone bosons eaten by $W_\mu^{(j,k)}$, and to the orthogonal states $\tilde{\eta}^{(j,k)a}$ ($a = 1, 2, 3$) which form a tower of physical spin-0 particles. For a detailed discussion of this mechanism, we refer the reader to Section 6 of Ref. [11]. The masses of these Higgs KK modes may be parametrized as

$$M_{h^{(j,k)}} = M_{j,k}\left(1 + \frac{2g^2}{N_c g_s^2} A_H C^G_{j,k} + \frac{M_h^2}{2M_{j,k}^2}\right),$$
$$M_{\tilde{\eta}^{(j,k)}} = M_{j,k}\left(1 + \frac{2g^2}{N_c g_s^2} A_{\tilde{\eta}} C^G_{j,k} + \frac{M_W^2}{2M_{j,k}^2}\right), \qquad (2.19)$$

where we assumed that the Higgs boson mass M_h is small enough compared to the compactification scale such that the $(M_h/M_{j,k})^4$ corrections may be ignored. In the limit $M_h \ll 1/R$, the KK modes of the Higgs boson, $h^{(j,k)}$, and of the three eaten Nambu-Goldstone bosons, $\tilde{\eta}^{(j,k)\pm}$ and $\tilde{\eta}^{(j,k)3}$, form a degenerate $SU(2)_W$ doublet at each KK level, which we denote by $H^{(j,k)}$.

In this paper we are interested in the KK-parity even states, which can be singly produced at colliders, as we will see in the next section. It will be useful to have the mass shift formulae (2.11) and (2.12) that follow from the one-loop results, Eqs. (2.7)–(2.10), applied to the standard model gauge group and field content. For the gluon vector modes, and for the $SU(2)_W$-doublet and -singlet quark modes, Q_+ and Q_- respectively, we find

$$A_G = \frac{13}{3}, \qquad A_{Q_+} = \frac{20}{9} + \frac{1}{4g_s^2}\left(\lambda_{q_L}^2 + 5g^2 + \frac{5}{27}g'^2\right),$$
$$A_{Q_-} = \frac{20}{9} + \frac{1}{g_s^2}\left(\frac{1}{2}\lambda_{q_R}^2 + \frac{5}{12}y_{q_R}^2 g'^2\right), \qquad (2.20)$$

where y_f are the hypercharges of the quarks and leptons, normalized such that the quark doublets have $y = 1/3$. Here λ_{q_L} and λ_{q_R} are the Yukawa couplings to the Higgs doublet (given by $\lambda_{b_L} = \lambda_{t_L} = \lambda_{t_R} \equiv \lambda_t \simeq 1$, and negligible for the other flavors). Note that the top Yukawa gives a positive contribution so that the third generation Q^3 and U^3 KK modes are heavier than those of the first two generations. The positive contribution to the mass shifts due to Yukawa couplings is special to six dimensions, and is related to the existence of two 6D chiralities, both of which must be involved in the Yukawa interaction (notice that in 5D the Yukawa couplings give a negative contribution to the mass shifts [6]). Note also that the KK gluons are heavier than the KK quarks. However, as we stressed before, for strongly interacting particles the one-loop results should be taken only as indicative of the size of the mass shifts. Although a situation where the KK quarks are heavier than the KK gluons is possible, we will assume that higher order contributions do not change the hierarchy of masses found at one-loop.

For the electroweak gauge bosons, we get

$$A_W = \frac{85}{24}, \qquad A_B = -\frac{83}{12}, \qquad (2.21)$$

while the leptons have

$$A_L = \frac{15}{8}\left(1 + \frac{g'^2}{3g^2}\right), \qquad A_E = 5, \qquad (2.22)$$

so that the $SU(2)_W$ gauge boson modes are heavier than the lepton modes.

For the spinless adjoints the mass shifts arise from the second term in Eq. (2.5) and the analogous terms in the electroweak sector. As shown in [11], the KK-expansion of the extra-dimensional field strength, F_{45}, defines gauge invariant linear combinations of A_4 and A_5 that are orthogonal to the would-be Nambu-Goldstone bosons eaten by the vector modes at each KK level. Thus, only these gauge invariant degrees of freedom, that we call spinless adjoints, get a mass shift from the localized terms, given in the third equation of (2.11). We obtain the following values for the parameters defined by Eqs. (2.17):

$$A_{G_H} = 1, \qquad A_{W_H} = -\frac{17}{8}, \qquad A_{B_H} = -\frac{153}{4}. \qquad (2.23)$$

Note that the (1,1) $SU(3)_C$ spinless adjoints receive a positive contribution to their masses, but are typically lighter than the (1,1) quarks. Similarly, the electroweak spinless adjoints are lighter than the (1,1) leptons. Their masses are driven down by the contribution due to the fermions.

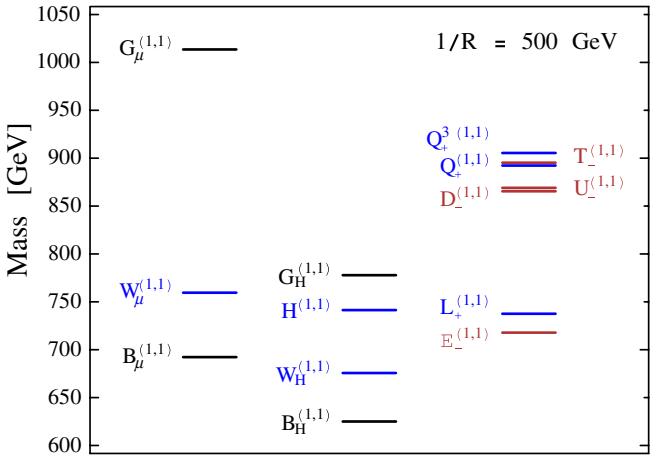

FIG. 1 (color online). Mass spectrum of the (1,1) level for $1/R = 500$ GeV. Electroweak symmetry breaking effects are small, and have not been included.

Finally, the parameters that control the KK Higgs masses in Eq. (2.19) are given by

$$A_H \simeq A_{\tilde{\eta}} \simeq \frac{33}{32} + \frac{\lambda_t^2}{2g^2}, \tag{2.24}$$

where we have not included the contributions from Higgs self-interactions and from $U(1)_Y$ interactions.

The mass spectrum of the (1,1) modes is shown in Fig. 1 for $1/R = 500$ GeV. Higher-loop contributions involving colored KK modes may be important (see the end of Section II B), and may shift the mass spectrum. This uncertainty is larger than corrections coming from the running of the coupling constants, or electroweak symmetry breaking. We ignored these effects in Fig. 1, and we used some rough estimates for the couplings at the scale $M_{1,1} = \sqrt{2}/R$: $(g/g_s)^2 = 0.34$, $(g'/g_s)^2 = 0.10$, $(\lambda_t/g_s)^2 = 0.8$,

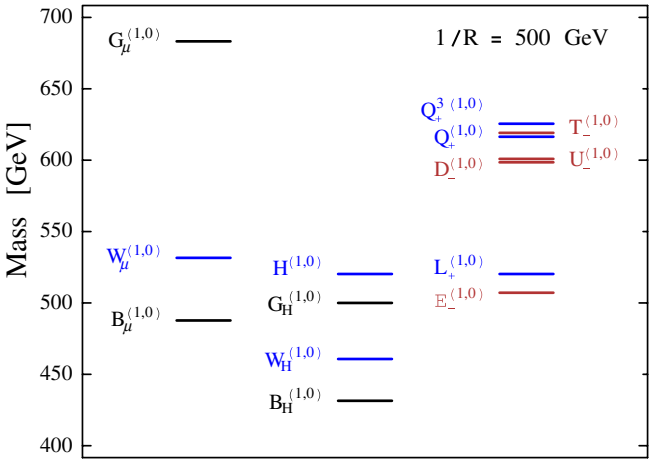

FIG. 2 (color online). Mass spectrum of the (1,0) level. The lightest KK particle is the $B_H^{(1,0)}$ spinless adjoint.

$C^G = 0.1$. We also assumed that the Higgs boson is much lighter than the compactification scale.

We also point out here that at the (1,0) level, the mass corrections to the electroweak spinless adjoints are also negative. The mass correction to the (1,0) $SU(3)_C$ spinless adjoints happens to vanish at one-loop for the standard model field content, but one should keep in mind that multiloop contributions are expected to be important for the strongly interacting particles. The corresponding mass shifts for the spin-1 particles are positive for the (1,0) gluons, and negative for the (1,0) W and B vector modes. In fact, it is interesting that the lightest KK particle is predicted to be the spinless hypercharge mode, $B_H^{(1,0)}$. Thus, in contrast to the case of five dimensions, the natural dark matter candidate has spin-0. The mass spectrum of the (1,0) modes is shown in Fig. 2 for $1/R = 500$ GeV.

D. KK-number-violating interactions

The Z_2^{KK} symmetry implies that for any interaction among KK modes the sum over all j and k numbers should be even. In particular, interactions involving two zero modes and a (j, k) mode with $j \geq 1$ and $j + k$ even is allowed. Such an interaction is not generated at tree level by bulk interactions, but arises due to the localized operators.

To be concrete, the effective 4D, KK-number-violating couplings between zero-mode quarks and massive KK gluons are given by

$$g_s C_{j,k}^{qG} (\bar{q}\gamma^\mu T^a q) G_\mu^{(j,k)a}, \tag{2.25}$$

where $C_{j,k}^{qG}$ are real dimensionless parameters, T^a are the $SU(3)_C$ generators in the fundamental representation, g_s is the QCD gauge coupling, and q stands for any of the standard model quarks. The strength of the couplings to zero-mode fermions is controlled by the kinetic terms localized at the fixed points, and contained in $\mathcal{L}_1$ and $\mathcal{L}_2$ in Eq. (2.3). Their dimensionless coefficients ultimately determine the strength of the KK-number-violating couplings of fermions to gauge bosons. In terms of the coefficients defined in Eqs. (2.4) and (2.5), $C_{j,k}^{qG}$ is given to lowest order in the localized terms by

$$C_{j,k}^{qG} = -\frac{1}{2}\overline{\delta Z}_{G^{(j,k)}} + \frac{1}{2}\overline{\delta Z}_{q^{(j,k)}} - \frac{1}{2}\overline{\delta Z}'_{q^{(j,k)}}, \tag{2.26}$$

where it is understood that $G^{(j,k)}$ is KK-parity even [i.e. $j + k$ is even], but not the zero-mode, and

$$\begin{aligned}
\overline{\delta Z}_{q^{(j,k)}} &= \frac{1}{(\pi M_s R)^2}(2C_{1q} + (-1)^j C_{2q}), \\
\overline{\delta Z}'_{q^{(j,k)}} &= \frac{2}{(\pi M_s R)^2}\,\mathrm{Re}(2C'_{1q} + (-1)^j C'_{2q}), \\
\overline{\delta Z}_{G^{(j,k)}} &= \frac{1}{(\pi M_s R)^2}(2C_{1G} + (-1)^j C_{2G}).
\end{aligned} \tag{2.27}$$

Notice that when both j and k are even we can write Eq. (2.26) in terms of the mass shifts given in Eq. (2.11) as

$$C_{j,k}^{qG} = \frac{\delta M_{G^{(j,k)}}}{M_{j,k}} - \frac{\delta M_{q^{(j,k)}}}{M_{j,k}}, \qquad j, k \text{ even}. \tag{2.28}$$

However, when both j and k are odd the above relation does not hold (unless there are no terms induced at $(x^4, x^5) = (0, \pi R)$, i.e. $C_{1q} = C'_{1q} = C_{1G} = 0$). In this case, the above interactions depend on a different combination of the coefficients in $\mathcal{L}_1$ and $\mathcal{L}_2$ than the KK mass shifts and are, effectively, independent parameters.

As mentioned above, the coefficients of the localized operators receive contributions from physics at the cutoff M_s, and run logarithmically below M_s due to bulk loop effects. The contribution to the localized couplings from physics between the scales M_s and $\mu < M_s$ is of the order of $(g^2 N_c/16\pi^2)\ln(M_s^2/\mu^2)$. This contribution is enhanced compared to the bare one by a logarithmic factor. Based on these NDA estimates, Eqs. (2.26) and (2.27) give the values of the parameters $C_{j,k}^{qG}$ at the scale of the KK-mode mass $M_{j,k}$:

$$C_{j,k}^{qG} = \xi_q^G C_{j,k}^G, \tag{2.29}$$

where ξ_q^G is a dimensionless parameter of order unity, and $C_{j,k}^G$ was defined in Eq. (2.14).

The localized operators at the cutoff scale may be flavor dependent. Their contributions to the C^{qG} coefficients are not shown in Eq. (2.14) because they are not enhanced by the logarithmic factor. Nevertheless, Eq. (2.6) implies that the logarithmic factor is at most as large as $\ln(M_s R)^2 \approx 4.6$, and therefore the flavor dependent operators may lead to large flavor-changing neutral processes. In order to suppress these, the physics above the cutoff scale must possess some approximate flavor symmetry.

The KK spinless adjoints interact with the zero-mode quarks only via dimension-5 or higher operators:

$$\frac{g_s \tilde{C}_{j,k}^{qG}}{M_{j,k}} (\bar{q}\gamma^\mu T^a q) D_\mu G_H^{(j,k)a}, \tag{2.30}$$

where $\tilde{C}_{j,k}^{qG}$ are real dimensionless parameters, and D_μ is the gauge covariant derivative. The largest contributions to these coefficients arise from the quark and spinless adjoint kinetic and mass mixing effects associated with the localized kinetic terms of Eqs. (2.4) and (2.5). There is also a subdominant finite direct vertex contribution, suppressed by a logarithm compared to the mixing effects. According to NDA, the direct bare contributions from localized operators to the interaction (2.30) are of order $(g_s^2 N_c/16\pi^2)^2$, and are therefore negligible compared to the contributions due to mixing effects. It is important to notice that the vertex (2.30) is proportional to the quark masses, as can be seen by integrating by parts and using the fermion equations of motion. As a result, the spinless adjoints decay almost exclusively into top quarks. This observation also implies that the coupling for direct production of the spinless states is negligible, being suppressed by the u or d-quark masses. However, the spinless adjoints can be easily produced in the decays of KK quarks or leptons, as we discuss in the next section.

Dimension-4 operators which couple a single spinless adjoint to one or two zero-mode gluons are forbidden by the unbroken gauge invariance associated with the zero-mode gauge boson. Naively, a spinless adjoint may couple to zero-mode gluons via the dimension-5 operator

$$\frac{1}{M_{j,k}} \mathrm{Tr}(G^{\mu\nu} G_{\mu\nu} G_H^{(j,k)}) \tag{2.31}$$

or the analogous operator involving a dual field strength. However, these operators vanish because the trace over three generators T^a, T^b, T^c in the adjoint representation is proportional to the antisymmetric structure constant f^{abc}, and two indices are contracted with identical gluon field strengths. On the other hand, the operator obtained by replacing one of the gluon field strengths in (2.31) by the field strength of a KK gluon need not vanish, and generates a coupling of a spinless adjoint to a KK gluon and a gluon zero mode.

Higher-dimension operators coupling the hypercharge spinless adjoint to two spin-1 fields, e.g., $\mathrm{Tr}(G^{\mu\nu} G_{\mu\nu} B_H^{(j,k)})$ or $B^{\mu\nu} B_{\mu\nu} B_H^{(j,k)}$, could be present. Interestingly, the one-loop contributions to their coefficients vanish. This is because $B_H^{(j,k)}$ couples to fermions via an axial-scalar coupling so that the relevant triangle diagrams are proportional to the corresponding gauge anomaly coefficients, which are canceled.

The $W_\mu^{(j,k)a}$ KK modes couple to zero-mode fermions through

$$g C_{j,k}^{fW} (\bar{f}_L \gamma^\mu T_2^a f_L) W_\mu^{(j,k)a}, \tag{2.32}$$

where T_2^a are the $SU(2)_W$ generators, g is the 4D $SU(2)_W$ gauge coupling, and f are the quark and lepton fields of any generation. It is convenient to write the dimensionless parameters $C_{j,k}^{fW}$ as follows:

$$C_{j,k}^{qW} \equiv \xi_q^W C_{j,k}^G, \qquad C_{j,k}^{lW} \equiv \frac{2g^2}{g_s^2 N_c} \xi_l^W C_{j,k}^G. \tag{2.33}$$

Here, l stands for the $SU(2)_W$-doublet leptons. The ξ_q^W and ξ_l^W parameters are estimated via NDA to be of order unity.

Similarly, the $B_\mu^{(j,k)}$ KK modes couple to zero-mode quarks and leptons:

$$g' \frac{y_f}{2} C_{j,k}^{fB} (\bar{f}\gamma^\mu f) B_\mu^{(j,k)}, \tag{2.34}$$

where g' is the 4D $U(1)_Y$ gauge coupling, and y_f are the hypercharges of the quarks and leptons, normalized such that the quark doublets have $y = 1/3$. The $C_{j,k}^{fB}$ parameters

may be written in terms of other parameters $(\xi_q^B, \xi_l^B, \xi_e^B)$ expected to be of order unity:

$$C_{j,k}^{qB} \equiv \xi_q^B C_{j,k}^G, \qquad C_{j,k}^{lB} \equiv \frac{2g^2}{g_s^2 N_c}\xi_l^B C_{j,k}^G, \qquad C_{j,k}^{eB} \equiv \frac{g'^2}{g_s^2 N_c}\xi_e^B C_{j,k}^G. \tag{2.35}$$

So far we have parametrized the (0,0) (0,0), (j, k) couplings, using NDA as a guide to argue that certain parameters are expected to be of order unity. The explicit one-loop results, Eqs. (2.7)–(2.10), involve a $((j + k)/2, (k - j)/2)$ mode in the loop when $j \geq k$, and a $((j - k)/2, (j + k)/2)$ mode when $j < k$ [10]. For j and k even, there is also a one-loop contribution with a $(j/2, k/2)$ mode running in the loop. As a result, the (0,0) (0,0) (1,1) interaction is generated by a (1,0) loop, while the (0,0) (0,0) (2,0) interaction is generated by the sum of a (1,0) loop and a (1,1) loop. As we will see below, these interactions of KK modes beyond the (1,0) level with two zero-mode fields, have important phenomenological consequences. Also note that the leading contributions to these one-loop diagrams involve gluon and quark KK modes, and therefore are flavor independent. Electroweak KK modes induce some splitting between the couplings of the $SU(2)_W$-doublet and singlet quarks as well as between the up- and down-type quarks. Another effect is due to the Yukawa couplings to the Higgs doublet, and is notable only for the (t_L, b_L) and t_R quark fields.

If we use Eqs. (2.7)–(2.10) we find, in the case of 6D gauge fields A_α interacting with some 6D Weyl fermions f and 6D complex scalars s which have zero modes, that the ''renormalization'' constants (2.27) that determine the couplings of the (1,1) vector modes to zero-mode fermions via Eq. (2.26), are given by

$$\begin{aligned}
\overline{\delta Z}_{f^{(1,1)}} &= \left[-6\sum_A C_2(f) g_A^2 + \sum_i \lambda_i^2\right]\frac{1}{16\pi^2}\ln\left(\frac{M_s^2 R^2}{2}\right),\\
\overline{\delta Z}'_{f^{(1,1)}} &= \sum_i \lambda_i^2 \frac{1}{8\pi^2}\ln\left(\frac{M_s^2 R^2}{2}\right),\\
\overline{\delta Z}_{A^{(1,1)}} &= \left[-\frac{22}{3}C_2(A) + \frac{4}{3}\sum_f T(f) + \frac{2}{3}\sum_s T(s)\right] g_A^2 \frac{1}{16\pi^2}\\
&\quad \times \ln\left(\frac{M_s^2 R^2}{2}\right).
\end{aligned} \tag{2.36}$$

Applying this result to the standard model gauge group, we find the parameters introduced in Eq. (2.29),

$$\begin{aligned}
\xi_{q_L}^G &= 1 - \frac{1}{2g_s^2}\left(\frac{1}{3}\lambda_{q_L}^2 + \frac{3}{2}g^2 + \frac{1}{18}g'^2\right),\\
\xi_{q_R}^G &= 1 - \frac{1}{g_s^2}\left(\frac{1}{3}\lambda_{q_R}^2 + \frac{y_{q_R}^2}{4}g'^2\right).
\end{aligned} \tag{2.37}$$

Similarly, the parameters that control the $W_\mu^{(1,1)}$ couplings to zero-mode fermions are given by

$$\begin{aligned}
\xi_q^W &= -\frac{4}{3} - \frac{\lambda_q^2}{6g_s^2} + \frac{1}{36g_s^2}(11g^2 - g'^2),\\
\xi_l^W &= \frac{11}{24} - \frac{3g'^2}{8g^2}.
\end{aligned} \tag{2.38}$$

Note that in the above equations the hypercharge interaction give only small corrections, which for practical purposes may be neglected in what follows. However, in the case of the $B_\mu^{(1,1)}$ couplings to zero-mode fermions, the wave function renormalization of $B_\mu^{(1,1)}$ (more precisely, its mixing with $B_\mu^{(0,0)}$) is enhanced by the large number of fields, giving a relatively large contribution from the hypercharge interaction:

$$\begin{aligned}
\xi_{q_L}^B &= -\frac{4}{3} - \frac{1}{2g_s^2}\left(\frac{1}{3}\lambda_{q_L}^2 + \frac{3}{2}g^2 + \frac{83}{18}g'^2\right),\\
\xi_{q_R}^B &= -\frac{4}{3} - \frac{1}{g_s^2}\left[\frac{1}{3}\lambda_{q_R}^2 + \left(\frac{41}{18} + \frac{y_{q_R}^2}{4}\right)g'^2\right],\\
\xi_l^B &= -\frac{9}{8} - \frac{91g'^2}{24g^2},\\
\xi_e^B &= -\frac{59}{6}.
\end{aligned} \tag{2.39}$$

Note that the couplings of the spin-1 KK modes to the third generation quarks are somewhat enhanced due to the loops involving Higgs KK modes.

III. DECAYS OF THE (1,1) MODES

The 6D standard model outlined in the previous section leads to specific predictions for the properties of the KK modes. In this section we compute the branching fractions of the (1,1) modes, which are of special interest for collider phenomenology. We start by summarizing the information regarding the parameters that control the branching fractions, and then we discuss in turn each of the (1,1) modes.

A. Parameters

The most important parameter is $1/R$, which sets the overall scale of the KK mass spectrum. Lower limits on $1/R$ are set mainly by electroweak precision constraints and are likely to be in the 300–500 GeV range, based on the study from Refs. [4,16], where a different compactification of two extra dimensions has been considered. We emphasize that the limits from electroweak constraints are sensitive to higher-dimensional operators at the cutoff scale, and therefore are not nearly as robust as the limits that will be set by collider searches (see Sec. IV B).

The cutoff scale, M_s, is in principle another free parameter. However, it cannot be too close to $1/R$ because the effective field theory loses its validity, and it cannot be too far above $1/R$ because the effective field theory becomes nonperturbative. We use the NDA estimate given in Eq. (2.6): $M_s = 10/R$. Given that the physical observables

depend on the cutoff scale only logarithmically, this choice is not a source of large uncertainties.

The coefficients of the localized kinetic terms are all parameters beyond those in the standard model. They control the leading contributions to the mass splittings among the modes within a given KK level, as well as the KK-number-violating couplings, as discussed in the previous section. We note that there are two parameters per localized operator: one controls the strength of the operator at (0,0) and $(\pi R, \pi R)$, while the second one controls the strength at $(0, \pi R)$. It is important to notice that the mass shifts and KK-number-violating couplings depend on different linear combinations of these two parameters. Since in this paper we are mainly interested in the phenomenology of the (1,1) level, we may consider their masses and couplings as independent parameters. However, one should keep in mind that knowledge of these parameters imply definite relations for the masses and couplings of other states, such as the (1,0) modes.

The loop factor that controls the couplings of the (1,1) gluons to zero-mode quarks C^G is (we drop the $j = k = 1$ indices)

$$C^G = \frac{\alpha_s N_c}{4\pi} \ln\left(\frac{M_s^2 R^2}{2}\right) \simeq 0.1. \tag{3.1}$$

where we used the value of the strong coupling constant at a scale of about 1 TeV, $\alpha_s = 0.1$.

The $G_\mu^{(1,1)}$, $W_\mu^{(1,1)3}$, and $B_\mu^{(1,1)}$ particles have couplings to zero-mode fermions proportional to the parameters of order one ξ_q^G, ξ_q^W, ξ_l^W, ξ_q^B, ξ_l^B, and ξ_e^B, introduced in Eqs. (2.29), (2.33), and (2.35). We will keep the dependence on the ξ parameters explicit whenever possible, but for numerical results we use the one-loop values given in Eqs. (2.37), (2.38), and (2.39). One should emphasize that the decay widths and production cross sections depend quadratically on the ξ parameters. Therefore, the estimates for the ξ parameters, which for strongly interacting particles could be off by a factor as large as 2 or so, is a major source of uncertainty in the predictions of this model. Barring unexpectedly large bare contributions, the ξ parameters associated with the weakly interacting particles are expected to be more reliable. In addition, one should keep in mind that the flavor independence of the (1,1) couplings may be only approximate: the localized operators induced by physics at the cutoff scale may be flavor dependent (as discussed in Sec. II, this is a subdominant effect because the coefficients of these operators are not enhanced by a logarithmic factor).

Other parameters control the mass splittings among various (1,1) states. These are also determined by the coefficients of the localized operators, so that they are related to C^G as shown in Eqs. (2.13)–(2.19). We will keep the dependence on the coefficients A_G, A_{G_H}, A_{Q_+}, A_{Q_-}, A_W, A_{W_H}, A_L, A_B, A_{B_H}, A_E, and A_H explicit in our analytic results, while in the numerical analysis we will use the values given in Eqs. (2.20)–(2.23).

B. Branching fractions of the B_μ (1,1)-mode

As we discussed in Sec. II C, $B_\mu^{(1,1)}$ is the lightest of the standard model KK excitations at the (1,1) level. Only its spinless partner, $B_H^{(1,1)}$, is expected to be lighter. Thus, $B_\mu^{(1,1)}$ can only decay into zero modes or into $B_H^{(1,1)}$ plus zero modes. We consider first the decays into zero modes only. Their widths may be computed in terms of the couplings given in Eqs. (2.34). The decay width into $q\bar{q}$, with $q = u$, d, s, c, is given by

$$\Gamma(B_\mu^{(1,1)} \to q\bar{q}) = \Gamma_0^B[(\xi_{q_L}^B)^2 + 8(\xi_{u_R}^B)^2 + 2(\xi_{d_R}^B)^2], \tag{3.2}$$

where we summed over the four $q\bar{q}$ flavors, and we defined

$$\Gamma_0^B \equiv \frac{\alpha}{18\cos^2\theta_w}(C^G)^2 M_{B^{(1,1)}}. \tag{3.3}$$

Here θ_w is the weak mixing angle, and α is the electromagnetic coupling constant at a scale of order $1/R$. The decay widths into $t\bar{t}$ and $b\bar{b}$ are as follows:

$$\Gamma(B_\mu^{(1,1)} \to t\bar{t}) = \Gamma_0^B\left[\frac{1}{4}(\xi_{t_L}^B)^2 + 4(\xi_{t_R}^B)^2\right]\left(1 - \frac{m_t^2}{M_{B^{(1,1)}}^2}\right) \times \left(1 - \frac{4m_t^2}{M_{B^{(1,1)}}^2}\right)^{1/2}, \tag{3.4}$$

$$\Gamma(B_\mu^{(1,1)} \to b\bar{b}) = \Gamma_0^B\left[\frac{1}{4}(\xi_{t_L}^B)^2 + (\xi_{d_R}^B)^2\right].$$

Note that we have neglected the QCD corrections and the b-quark mass.

The leptonic decays of $B_\mu^{(1,1)}$ are induced by the 6D electroweak interactions:

$$\Gamma(B_\mu^{(1,1)} \to \ell^+\ell^-) = \Gamma_0^B \frac{\alpha^2}{3\alpha_s^2 \sin^4\theta_w}[(\xi_l^B)^2 + (\xi_e^B)^2 \tan^4\theta_w],$$

$$\Gamma(B_\mu^{(1,1)} \to \nu\bar{\nu}) = \Gamma_0^B \frac{\alpha^2}{\alpha_s^2 \sin^4\theta_w}(\xi_l^B)^2, \tag{3.5}$$

where $\ell = e$, μ, τ, and there is no sum over the three charged lepton pairs, while the decay width into $\nu\bar{\nu}$ is summed over the three neutrino flavors.

There are also 3-body decays, $B_\mu^{(1,1)} \to B_H^{(1,1)}\ell^+\ell^-$ through an off-shell (1,1) lepton. The decay that proceeds through off-shell $SU(2)_W$-singlet leptons dominates because of their larger hypercharge. In the limit that $B_\mu^{(1,1)}$ and $B_H^{(1,1)}$ are almost degenerate, $M_B - M_{B_H} \ll M_B$, we find

$$\Gamma(B_\mu^{(1,1)} \to B_H^{(1,1)} \ell^+ \ell^-) \approx \frac{\alpha^2 M_{E^{(1,1)}}^2 (M_{B^{(1,1)}} - M_{B_H^{(1,1)}})^4}{\pi \cos^4\theta_w M_{B^{(1,1)}} (M_{E^{(1,1)}}^2 - M_{B_H^{(1,1)}}^2)^2} \approx \Gamma_0^B \frac{\alpha^3 (A_B - A_{B_H})^4}{2\pi\alpha_s^2 \cos^6\theta_w (A_E - A_{B_H})^2}. \tag{3.6}$$

In the second equality we used the parametrizations of the masses given in Sec. II C, and expanded to lowest order in the mass shifts. Although for the 1-loop values of A_B, A_{B_H} and A_L given in Sec. II C there is a considerable "resonant" enhancement, it is not enough to overcome the phase-space suppression and we find that this partial decay width is at least 1 order of magnitude smaller than the two-body decay into leptons of Eq. (3.5). Given that the two-body leptonic decay is much smaller than the two-body decay into $q\bar{q}$, we conclude that $B_\mu^{(1,1)}$ is almost "leptophobic" (this term was coined in Ref. [17]).

The decays of $B_\mu^{(1,1)}$ into $B_H^{(1,1)}$ and a Z boson or a photon could proceed through higher-dimension operators similar to those discussed after Eq. (2.31). Such effects are suppressed compared to the two-body decays discussed above, and therefore we neglect them. Note, however, that the decays of the first-level vector mode $B_\mu^{(1,0)}$ through such higher-dimension operators could be phenomenologically relevant.

The $B_\mu^{(1,1)}$ total width, in the limit $(m_t R)^2 \ll 1$ and neglecting (3.6), is given approximately by

$$\Gamma_B = \Gamma_0^B \left\{ (\xi_{q_L}^B)^2 + 8(\xi_{u_R}^B)^2 + 3(\xi_{d_R}^B)^2 + \frac{1}{2}(\xi_{t_L}^B)^2 + 4(\xi_{t_R}^B)^2 + \frac{\alpha^2}{\alpha_s^2}\left[\frac{2(\xi_l^B)^2}{\sin^4\theta_w} + \frac{(\xi_e^B)^2}{\cos^4\theta_w} \right] \right\}. \tag{3.7}$$

We compute the ξ parameters from Eqs. (2.39), using $\alpha = 1/127$, $\sin^2\theta_w = 0.23$, $\alpha_s = 0.1$, and $\lambda_t = 1$, which gives $(g/g_s)^2 = 0.34$, $(g'/g_s)^2 = 0.10$, and $(\lambda_t/g_s)^2 = 0.8$. Note that these values for the coupling constants are our rough estimates of their average values at a scale $M_{1,1}$ in the range ~0.4–1 TeV. In order to use more precise values for the coupling constants one would need to compute the changes in their running due to all lighter particles, including the (1,0) modes. However, the masses of the colored (1,0) modes may get relatively large corrections from localized operators at the cutoff scale, so that we cannot include a precise scale dependence of the coupling constants.

For quarks, the resulting values of the ξ parameters are of order unity, as expected: $\xi_{q_L}^B \simeq -1.8$, $\xi_{u_R}^B \simeq \xi_{d_R}^B \simeq -1.6$, $\xi_{t_L}^B \simeq -2.0$, $\xi_{t_R}^B \simeq -1.9$. For leptons, the couplings are somewhat enhanced as discussed in subsection II D: $\xi_l^B \simeq -2.3$, $\xi_e^B \simeq -9.8$. The branching fractions computed with these parameters are 59% into dijets (not including b jets), 30% into $t\bar{t}$, 7.1% into $b\bar{b}$, 0.9% for each of the e^+e^-, $\mu^+\mu^-$ and $\tau^+\tau^-$ pairs, and 1.1% for invisible decays. The total width is $\Gamma_B \simeq 2.4 \times 10^{-4} M_{B^{(1,1)}}$, so $B_\mu^{(1,1)}$ is an extremely narrow resonance.

For larger values of $m_t R$, the branching fraction into $t\bar{t}$ is reduced as in Eq. (3.4), while the other branching fractions are somewhat increased (see the values in Table III of Sec. III D for $1/R = 500$ GeV).

C. Branching fractions of the W_μ^3 (1,1)-mode

The width of the $W_\mu^{(1,1)3}$ decay to quarks depends on the couplings ξ_q^W defined in Eq. (2.33):

$$\Gamma(W_\mu^{(1,1)3} \to q\bar{q}) = 4\Gamma_0^W (\xi_q^W)^2, \tag{3.8}$$

where $q = u$, d, s, c, we summed over these four $q\bar{q}$ flavors, and we ignored QCD corrections. Here we defined

$$\Gamma_0^W \equiv \frac{\alpha}{8\sin^2\theta_w} (C^G)^2 M_{W^{(1,1)}}. \tag{3.9}$$

For $t\bar{t}$ and $b\bar{b}$ final states we find

$$\Gamma(W_\mu^{(1,1)3} \to t\bar{t}) = \Gamma_0^W (\xi_t^W)^2 \left(1 - \frac{m_t^2}{M_{W^{(1,1)}}^2}\right)\left(1 - \frac{4m_t^2}{M_{W^{(1,1)}}^2}\right)^{1/2},$$
$$\Gamma(W_\mu^{(1,1)3} \to b\bar{b}) = \Gamma_0^W (\xi_t^W)^2. \tag{3.10}$$

The leptonic widths of $W_\mu^{(1,1)3}$ are the same for each neutrino flavor or left-handed charged lepton:

$$\Gamma(W_\mu^{(1,1)3} \to e_L^+ e_L^-) = \Gamma_0^W (\xi_l^W)^2 \frac{4\alpha^2}{27\alpha_s^2 \sin^4\theta_w}. \tag{3.11}$$

If the $W_\mu^{(1,1)3}$ boson is heavier than the (1,1) leptons, then it may also decay into a (1,1) lepton and a zero-mode lepton. In fact this is the case for the values of the masses given in Sec. II. Summing over the decay widths into leptons and antilepton doublets of the three generations, we obtain

$$\Gamma\left(W_\mu^{(1,1)3} \to \sum L^{(1,1)} l\right) = \frac{\alpha M_{W^{(1,1)}}}{2\sin^2\theta_w}\left(1 - \frac{M_{L^{(1,1)}}^2}{M_{W^{(1,1)}}^2}\right)^2 \times \left(1 + \frac{M_{L^{(1,1)}}^2}{2M_{W^{(1,1)}}^2}\right). \tag{3.12}$$

To first order in the mass shifts shown in Eqs. (2.16) and (2.18), we find

$$\Gamma\left(W_\mu^{(1,1)3} \to \sum L^{(1,1)} l\right) \simeq \Gamma_0^W \frac{32\alpha^2 (A_W - A_L)^2}{3\alpha_s^2 \sin^4\theta_w}. \tag{3.13}$$

Adding these decay modes to the ones into zero modes, we find the total width of $W_\mu^{(1,1)3}$ in the $(m_t R)^2 \ll 1$ limit:

$$\Gamma_W = \Gamma_0^W \Big\{ 4(\xi_q^W)^2 + (\xi_l^W)^2 \Big(2 - \frac{3m_t^2}{M^2_{W^{(1,1)}}}\Big) + \frac{8\alpha^2}{9\alpha_s^2 \sin^4\theta_w}[(\xi_l^W)^2 + 12(A_W - A_L)^2] \Big\}. \quad (3.14)$$

Using the ξ parameters from Eq. (2.38), $\xi_q^W \simeq -1.2$, $\xi_l^W \simeq 0.35$ and $\xi_t^W \simeq -1.4$, and the A parameters from Eq. (2.22), $A_W - A_L \simeq 1.5$, we find the branching fractions into $t\bar{t}$,

$$\mathrm{Br}\,(W_\mu^{(1,1)3} \to t\bar{t}) \simeq 15\% \Big(1 - \frac{2.6 m_t^2}{M^2_{W^{(1,1)}}}\Big), \quad (3.15)$$

and the decays that preserve KK number,

$$\mathrm{Br}\Big(W_\mu^{(1,1)3} \to \sum L^{(1,1)} l\Big) \simeq 22\% \Big(1 + \frac{0.44 m_t^2}{M^2_{W^{(1,1)}}}\Big), \quad (3.16)$$

For $m_t^2 \ll M^2_{W^{(1,1)}}$, the $W_\mu^{(1,1)3}$ has branching fractions of 48% into dijets (not including the b quark), 15% into $b\bar{b}$, 0.02% into each of the e^+e^-, $\mu^+\mu^-$ and $\tau^+\tau^-$ pairs, and 0.06% for invisible decays. Including the next order in the $m_t^2/M^2_{W^{(1,1)}}$ expansion, these branching fractions have the same m_t dependence as in Eq. (3.15). The $W_\mu^{(1,1)3}$ is almost as narrow as $B_\mu^{(1,1)}$, with a total width $\Gamma_W \simeq 10^{-3} M_{W^{(1,1)}}$.

D. Quark and lepton (1,1)-mode branching fractions

We assume, motivated by the 1-loop mass-shifts given in subsection II C, that the spinless adjoints, $G_H^{(1,1)}$, $W_H^{(1,1)}$, and $B_H^{(1,1)}$, are lighter than the (1,1)-quarks. In this case, the KK quarks can decay into both vector and spinless modes, via the KK-number preserving gauge interactions given in [11].

The $SU(2)_W$-doublet (1,1) quarks can decay into a zero-mode quark plus a $W_\mu^{(1,1)3}$ or $W_\mu^{(1,1)\pm}$ gauge boson, each with a partial decay width given by

$$\Gamma(Q_+^{(1,1)} \to W_\mu^{(1,1)i} q_L) = \frac{\alpha M_{Q_+^{(1,1)}}}{16 \sin^2\theta_w} \Big(1 - \frac{M^2_{W^{(1,1)}}}{M^2_{Q_+^{(1,1)}}}\Big)^2 \times \Big(1 + \frac{M^2_{Q_+^{(1,1)}}}{2M^2_{W^{(1,1)}}}\Big), \quad (3.17)$$

where we neglected the final quark mass. When the final state includes the top quark, as for $Q_L^{3(1,1)} \to W_\mu^{(1,1)i} t_L$ with $i = \pm, 3$, this approximation may not be valid. In fact, for the 1-loop masses of Sec. II C, these decays are closed for $1/R \sim 650$ GeV, and are phase space suppressed if the compactification scale is not much higher. We will neglect these decay channels in the following, although they could be important at the LHC, where compactification scales well above this limit can be probed.

Both the $SU(2)_W$-doublet and singlet (1,1) quarks may decay into $B_\mu^{(1,1)}$ and a zero-mode quark with a decay width of

$$\Gamma(Q^{(1,1)} \to B_\mu^{(1,1)} q) = \frac{y_q^2 \alpha M_{Q^{(1,1)}}}{16 \cos^2\theta_w} \Big(1 - \frac{M^2_{B^{(1,1)}}}{M^2_{Q^{(1,1)}}}\Big)^2 \times \Big(1 + \frac{M^2_{Q^{(1,1)}}}{2M^2_{B^{(1,1)}}}\Big), \quad (3.18)$$

where y_q is the hypercharge of the quark q (normalized such that $y_{u_R} = 4/3$).

Given that the quark (1,1) modes appear to be heavier than the spinless (1,1) gluon, the decay into a $G_H^{(1,1)}$ and a jet has a rather large width:

$$\Gamma(Q^{(1,1)} \to G_H^{(1,1)} q) = \frac{\alpha_s}{6} M_{Q^{(1,1)}} P\Big(\frac{M_{G_H^{(1,1)}}}{M_{Q^{(1,1)}}}, \frac{m_q}{M_{Q^{(1,1)}}}\Big), \quad (3.19)$$

where we defined the function

$$P(x, y) = (1 - x^2 + y^2)[(1 - x^2 - y^2)^2 - 4x^2 y^2]^{1/2}. \quad (3.20)$$

Note that the final-state quark is left-handed (right-handed) if the decaying (1,1) quark is an $SU(2)_W$-doublet (singlet). The $SU(2)_W$-doublet (1,1) quarks may also decay into a $W_H^{(1,1)}$ and a jet,

$$\Gamma(Q_+^{(1,1)} \to W_H^{(1,1)i} q_L) = \frac{\alpha}{32 \sin^2\theta_w} M_{Q_+^{(1,1)}} P\Big(\frac{M_{W_H^{(1,1)}}}{M_{Q_+^{(1,1)}}}, \frac{m_q}{M_{Q_+^{(1,1)}}}\Big). \quad (3.21)$$

We included here the dependence on the final-state quark mass, m_q, because the decay of the (1,1) b_L-quark, $B_+^{(1,1)}$, is sensitive to $m_t R$. Any of the (1,1) quarks may also decay into the hypercharge spinless adjoint and a jet with a width

$$\Gamma(Q^{(1,1)} \to B_H^{(1,1)} q) = \frac{y_q^2 \alpha}{32 \cos^2\theta_w} M_{Q^{(1,1)}} P\Big(\frac{M_{B_H^{(1,1)}}}{M_{Q^{(1,1)}}}, \frac{m_q}{M_{Q^{(1,1)}}}\Big). \quad (3.22)$$

The decay widths into the electroweak spinless adjoints are comparable to the weak decays of Eq. (3.17) or (3.18), while the decay into the spinless (1,1) gluon dominates. We base our estimates of the (1,1) quark branching fractions on the 1-loop corrected masses given in subsection II C, and summarize them in Table I.

The decays into the spinless adjoints, $G_H^{(1,1)}$, $W_H^{(1,1)3}$, and $B_H^{(1,1)}$, are very interesting since these subsequently decay most of the time into a pair of top quarks, giving rise to a potentially unique signal for these intrinsically 6D excitations. This is due to the fact that the coupling of the spinless adjoints to fermions is proportional to the fermion mass, as explained after Eq. (2.30).

As mentioned in Sec. II, the strongly interacting particles receive important contributions from multiloop ef-

TABLE I. Branching fractions (in percentage) into vector and spinless modes for the $SU(2)_W$-doublet quarks of the first two generations $Q_+^{(1,1)}$, for the (1,1) mode of the b_L-quark, $B_+^{(1,1)}$, and for the $SU(2)_W$-singlet quarks, $U_-^{(1,1)}$ and $D_-^{(1,1)}$. The branching fractions of the t quark (1,1) modes are strongly dependent on $m_t R$, and are not shown here. The phase-space suppression used for the decay $B_+^{(1,1)} \to W_H^{(1,1)-} t_L$ corresponds to $1/R = 0.5$ TeV.

Decay modes	$Q_+^{(1,1)}$	$B_+^{(1,1)}$	$U_-^{(1,1)}$	$D_-^{(1,1)}$
$G_H^{(1,1)} q$	41	58	61	86
$W_H^{(1,1)3} q$	8	11	—	—
$W_H^{(1,1)\pm} q$	17	14	—	—
$B_H^{(1,1)} q$	0.3	0.4	13	5
$W_\mu^{(1,1)3} q$	11	15	—	—
$W_\mu^{(1,1)\pm} q$	22	—	—	—
$B_\mu^{(1,1)} q$	0.9	1.1	26	9

TABLE II. Branching fractions (in percentage) into vector and spinless modes for the $SU(2)_W$-doublet leptons, $L^{(1,1)}$, and the $SU(2)_W$-singlet leptons, $E^{(1,1)}$.

Decay modes:	$W_H^{(1,1)\pm} l$	$W_H^{(1,1)3} l$	$B_H^{(1,1)} l$	$B_\mu^{(1,1)} l$
$L^{(1,1)}$	45	22	21	12
$E^{(1,1)}$	—	—	79	21

fects, and these could in principle make the spinless gluons, $G_H^{(1,1)}$, heavier than the (1,1) quarks, thus closing these decay channels. In that case, the $SU(2)_W$-doublet quarks would decay about 56% of the time into $W_\mu^{(1,1)} q_L$, 42% into $W_H^{(1,1)} q_L$, and the rest into $B_\mu^{(1,1)} q_L$ and $B_H^{(1,1)} q_L$. The $SU(2)_W$-singlet quarks would decay about 67% of the time into $B_\mu^{(1,1)} q_R$ and 33% into $B_H^{(1,1)} q_R$.

The (1,1) leptons can decay to the (1,1) modes of the electroweak gauge bosons or spinless adjoints. The decay widths are given by Eqs. (3.18), (3.21), and (3.22), with

TABLE III. Branching fractions of $W_\mu^{(1,1)3}$ and $B_\mu^{(1,1)}$ in percentage. The final states involving (1,1) bosons are due to cascade decays via a (1,1) lepton. The phase-space suppression of the decays into $t\bar{t}$ are computed for $1/R = 0.5$ TeV.

Decay modes	$W_\mu^{(1,1)3}$	$B_\mu^{(1,1)}$
$t\bar{t}$	13	26
$b\bar{b}$	16	8
dijet (no $b\bar{b}$)	52	62
$\sum \ell^+\ell^-$	0.05	3
$\nu\bar{\nu}$	0.05	1
$W_H^{(1,1)3}$ + leptons	4	—
$W_H^{(1,1)\pm}$ + leptons	9	—
$B_H^{(1,1)}$ + leptons	4	—
$B_\mu^{(1,1)}$ + leptons	2	—

$M_{Q^{(1,1)}}$ replaced by $M_{L^{(1,1)}}$, and y_q replaced by y_l. Using the one-loop results for the various masses given in subsection II C, we find the branching fractions summarized in Table II.

Combining the $W_\mu^{(1,1)3}$ branching fractions into a (1,1) lepton and a zero-mode lepton with the $L^{(1,1)}$ branching fractions, leads to the cascade decays of $W_\mu^{(1,1)3}$ into (1,1) bosons shown in Table III. Given that $W_H^{(1,1)3}$ and $B_H^{(1,1)}$ decay almost exclusively into $t\bar{t}$ pairs, about 21% of the $W_\mu^{(1,1)3}$ decays lead eventually to $t\bar{t}$ pairs.

E. Branching fractions of the gluon (1,1)-mode

The decays of $G_\mu^{(1,1)}$ that preserve KK numbers are into $U_{-_R}^{(1,1)} \bar{U}_R$, $\bar{U}_{-_R}^{(1,1)} u_R$, $U_{+_L}^{(1,1)} \bar{U}_L$, $\bar{U}_{+_L}^{(1,1)} u_L$, and the analogous pairs of the other five quark flavors. The partial widths for these decays are given by

$$\Gamma(G_\mu^{(1,1)} \to U_{-_R}^{(1,1)} \bar{U}_R) \simeq \frac{\alpha_s}{12} M_{G^{(1,1)}} \left(1 - \frac{M^2_{U^{(1,1)}_-}}{M^2_{G^{(1,1)}}}\right)^2 \times \left(1 + \frac{M^2_{U^{(1,1)}_-}}{2M^2_{G^{(1,1)}}}\right) \tag{3.23}$$

and analogous expressions for the other (1,1) quarks. Given the approximate degeneracy of the gluon and quark KK modes, the above decays are phase-space suppressed, and are in competition with the decay into a quark-antiquark pair, which is suppressed by the small KK-number-violating couplings:

$$\Gamma(G_\mu^{(1,1)} \to q\bar{q}) \simeq \frac{\alpha_s}{12} (C^G)^2 [(\xi^G_{q_L})^2 + (\xi^G_{q_R})^2] \times M_{G^{(1,1)}} \left(1 - \frac{3m_q^2}{M^2_{G^{(1,1)}}}\right), \tag{3.24}$$

where there is no flavor sum over the $q\bar{q}$ pairs. The decay into two gluons is also allowed [12], but even further suppressed.

Using the parametrization for the (1,1)-mode masses shown in Eqs. (2.13) and (2.15), assuming for the moment that all quark (1,1) modes are degenerate, and expanding for simplicity in $A_G C^G$, we find the total width of $G_\mu^{(1,1)}$:

$$\Gamma_G \approx \alpha_s (C^G)^2 M_{G^{(1,1)}} \left\{ \frac{1}{12} [4(\xi^G_{q_L})^2 + 2(\xi^G_{u_R})^2 + 3(\xi^G_{d_R})^2 + 2(\xi^G_{t_L})^2 + (\xi^G_{t_R})^2] + 10(A_G - A_Q)^2 \right\}. \tag{3.25}$$

Here we have taken into account that the $G_\mu^{(1,1)}$ decays to a t quark and one of its (1,1) modes are kinematically forbidden for $1/R \sim 1$ TeV. For $(A_G - A_Q)$ of order unity, $G_\mu^{(1,1)}$ has a width of the order of a few percent of its mass. Given that the ξ_q^G coefficients are also expected to be of order unity, the decay into a (1,1)-mode quark and a zero-mode

quark dominates. For each flavor of $q\bar{q}$ pairs, the branching fractions is approximately given by

$$\mathrm{Br}\,(G_\mu^{(1,1)} \to q\bar{q}) \approx \frac{(\xi_{q_L}^G)^2 + (\xi_{q_R}^G)^2}{120(A_G - A_Q)^2}, \tag{3.26}$$

which typically leads to branching fractions of less than 1%.

The values of the ξ parameters given by Eqs. (2.37) are indeed of order unity: $\xi_{q_L}^G = 0.74$, $\xi_{u_R}^G = 0.95$, $\xi_{d_R}^G = 0.99$, $\xi_{t_L}^G = 0.61$, and $\xi_{t_R}^G = 0.69$. However, according to the estimates of Sec. II C, A_G has a rather large value of $13/3$, so that for more precision we compute the branching fractions without expanding in $A_G C^G$. Using the quark (1,1) masses given by Eqs. (2.15) and (2.20), we find that the $G_\mu^{(1,1)}$ decays approximately 96% of the time into a (1,1) mode quark and the corresponding zero-mode quark. These decays are split as follows: 35% into down-type $SU(2)_W$-singlets, 22% into u_R and c_R modes, 32% into doublets of the first two generations, and 6.3% into b_L modes. The subsequent decay of the (1,1) quark depends on its transformation properties under $SU(2)_W$, as discussed in Sec. III D. Using the branching fractions of the (1,1) quarks given in Table I, we find the branching fractions for the $G_\mu^{(1,1)}$ cascade decays and direct decays listed in Table IV. The total width is $\Gamma_G \simeq 3.7 \times 10^{-2} M_{G^{(1,1)}}$.

As mentioned in Sec. III D, the electrically-neutral spinless adjoints, $G_H^{(1,1)}$, $W_H^{(1,1)3}$ and $B_H^{(1,1)}$, decay most of the time into $t\bar{t}$ pairs. The additional possible two-jet final states coming from two gluons are forbidden due to the vanishing of the operators similar to the one shown in Eq. (2.31). Furthermore, about 21% of the $W_\mu^{(1,1)3}$ decays lead to $t\bar{t}$ pairs (see Sec. III D), while $B_\mu^{(1,1)}$ has a branching fractions of about 26% into $t\bar{t}$. The decays of $W_\mu^{(1,1)\pm}$ involving a (1,1) lepton yield some additional $t\bar{t}$ pairs.

TABLE IV. Branching fractions of $G_\mu^{(1,1)}$ in percentage. The final states involving (1,1) bosons are due to cascade decays via a (1,1) quark. With the exception of the decays into $W_{H,\mu}^{(1,1)\pm}$ and $t\bar{t}$, whose widths are computed for $1/R = 0.5$ TeV, the branching fractions are only mildly dependent on $1/R$.

Decay modes	$G_\mu^{(1,1)}$
$G_H^{(1,1)}$ + jets	60.5
$W_H^{(1,1)3}$ + jets	3.2
$W_H^{(1,1)\pm}$ + jets	6.1
$B_H^{(1,1)}$ + jets	4.8
$W_\mu^{(1,1)3}$ + jets	4.3
$W_\mu^{(1,1)\pm}$ + jets	7.0
$B_\mu^{(1,1)}$ + jets	9.3
$t\bar{t}$	0.5
$b\bar{b}$	0.8
Dijet (no $b\bar{b}$)	3.3

We therefore expect a significant fraction, of about 72%, of the vector gluon modes to produce $t\bar{t}$ events.

IV. SIGNALS AT THE TEVATRON

In the absence of boundary terms, the conservation of KK number implies that KK modes cannot be singly-produced. In addition, as pointed out in Ref. [5] for the 5D case, the nearly degenerate spectrum typically results in rather soft jets and lepton signals. However, KK-number-violating interactions such as those in Eqs. (2.4) and (2.5), while still preserving Z_2^{KK}, allow for the production of single (1,1) states through their interactions with zero modes. In what follows, we study the s-channel production of the (1,1) KK gluon $G_\mu^{(1,1)}$, as well as of the electroweak gauge bosons $W_\mu^{(1,1)3}$ and $B_\mu^{(1,1)}$. Their subsequent decays give rise to interesting signals at the Tevatron.

A. s-channel production of the (1,1) modes

Let us first consider the s-channel production of the gluon vector mode $G_\mu^{(1,1)}$ through the coupling to $q\bar{q}$ pairs given in Eq. (2.25). The differential cross section for the s-channel process $q\bar{q} \to G_\mu^{(1,1)} \to U_{-R}^{(1,1)} \bar{U}_R$ is given by

$$\begin{aligned}\frac{d\hat{\sigma}_G}{d(\cos\theta)} = \frac{\pi\alpha_s^2}{36\hat{s}^2}(C^G)^2 \frac{(\hat{s} - M_{Q^{(1,1)}}^2)^2}{(\hat{s} - M_{G^{(1,1)}}^2)^2 + M_{G^{(1,1)}}^2 \Gamma_G^2} \\ \times \{[\hat{s}(1-\cos\theta)^2 + M_{Q^{(1,1)}}^2 \sin^2\theta](\xi_{q_L}^G)^2 \\ + [\hat{s}(1+\cos\theta)^2 + M_{Q^{(1,1)}}^2 \sin^2\theta](\xi_{q_R}^G)^2\},\end{aligned} \tag{4.1}$$

where θ is the angle between the momenta of $U_{-R}^{(1,1)}$ and q, and $\hat{s}$ is the energy of the parton collision, both defined in the center-of-mass frame.

In the narrow width approximation, the parton-level cross section for the production of a (1,1) gluon takes a simple form:

$$\begin{aligned}\hat{\sigma}(q\bar{q} \to G_\mu^{(1,1)}) = \frac{4\pi^2\alpha_s}{9M_G}(C^G)^2[(\xi_{q_L}^G)^2 + (\xi_{q_R}^G)^2] \\ \times \delta(\sqrt{\hat{s}} - M_{G^{(1,1)}}).\end{aligned} \tag{4.2}$$

Integrating this partonic cross section over the parton distribution functions, we find the inclusive cross section. At the Tevatron, the total production cross section is given by

$$\begin{aligned}\sigma(p\bar{p} \to G_\mu^{(1,1)} X) = \frac{8\pi^2\alpha_s}{9s}(C^G)^2 \sum_q t_q(M_{G^{(1,1)}}^2/s) \\ \times [(\xi_{q_L}^G)^2 + (\xi_{q_R}^G)^2].\end{aligned} \tag{4.3}$$

To leading order in α_s,

$$t_q(z) = \int_z^1 \frac{dx}{x}[q(x)q(z/x) + \bar{q}(x)\bar{q}(z/x)]. \tag{4.4}$$

The parton distribution functions (PDF's) $q(x)$ and $\bar{q}(x)$ are evaluated at the scale $M_{G^{(1,1)}}/2$, and $\sqrt{s} = 1.96$ TeV in Run II. We use the CTEQ6 leading order PDF's [18], and a correction factor of $K = 1.3$ to approximate the next-to-leading order (NLO) QCD corrections. This approximation is often used in the case of Z' production (for a discussion of its accuracy, see Ref. [19]). Note that $W_\mu^{(1,1)3}$ and $B_\mu^{(1,1)}$ fall into this category, whereas $G_\mu^{(1,1)}$ production has different color flow, so that a slightly different K factor may be necessary in that case; we will not study this issue in what follows. The result is the solid line shown in Fig. 3.

We emphasize that this is only a rough estimate of the vector-mode production cross sections. We have not included several corrections: (i) the nonresonant process induced by a t-channel exchange of a (1,1) gluon which involves a single KK-number-violating interaction; (ii) s-channel production of a (1,1) gluon from gluon fusion, via dimension-6 operators (note that the $q\bar{q}$ initial state dominates at the Tevatron); (iii) exact NLO and next-to-next-to-leading order QCD corrections. However, we expect our estimate to be correct up to a factor of less than 2, which is sufficient for the purpose of deciding whether a search for (1,1) modes at the Tevatron is useful.

The production cross sections for the s-channel processes $q\bar{q} \to W_\mu^{(1,1)3}$, $B_\mu^{(1,1)} \to q'\bar{q}'$ may be computed in a similar fashion. The differential cross sections for these two processes are given by

$$\frac{d\hat{\sigma}_W}{d(\cos\theta)} = \frac{\pi\alpha^2 (C^G)^4}{128\sin^4\theta_w} (\xi_q^W \xi_{q'}^W)^2 f_{q'}(\cos\theta) \times \frac{\hat{s}}{(\hat{s} - M^2_{W^{(1,1)}})^2 + M^2_{W^{(1,1)}}\Gamma^2_W}, \tag{4.5}$$

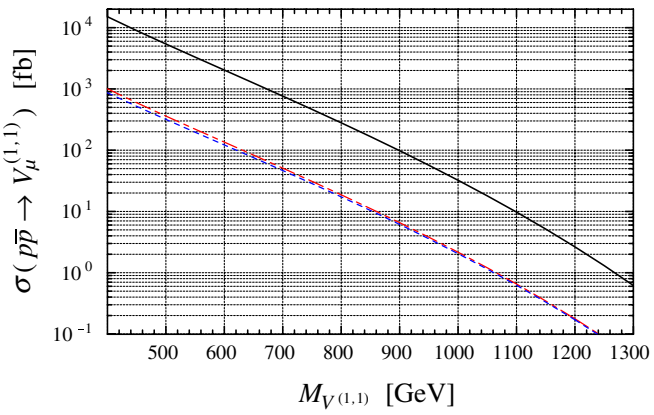

FIG. 3 (color online). Production cross sections for (1,1) vector modes in the s channel at the Tevatron, as a function of their mass. The solid line is for $G_\mu^{(1,1)}$, while the dashed and dotted (lowest) lines are for $W_\mu^{(1,1)3}$ and $B_\mu^{(1,1)}$, respectively, (accidentally, the cross sections for these two are close to each other such that they might not be distinguishable).

$$\frac{d\hat{\sigma}_B}{d(\cos\theta)} = \frac{\pi\alpha^2 (C^G)^4}{128\cos^4\theta_w} \frac{\hat{s}}{(\hat{s} - M^2_{B^{(1,1)}})^2 + M^2_{B^{(1,1)}}\Gamma^2_B} \times [(a_{q_L} a_{q'_L} + a_{q_R} a_{q'_R}) f_{q'}(\cos\theta) + (a_{q_R} a_{q'_L} + a_{q_L} a_{q'_R}) f_{q'}(-\cos\theta)], \tag{4.6}$$

where the function that encodes the angular distribution has the following form:

$$f_q(y) = (1+y)^2 - 2(1+4y+3y^2)\frac{m_q^2}{\hat{s}} + O(m_q^4/\hat{s}^2). \tag{4.7}$$

Note that we keep the dependence on the final-state quark masses, which is useful for the decay into $t\bar{t}$. The parameters a_{q_L}, $a_{q'_L}$, a_{q_R}, $a_{q'_R}$ are products of hypercharges and ξ parameters:

$$a_q = (\xi_q^B y_q)^2. \tag{4.8}$$

The parton-level production cross sections are given in the narrow width approximation by

$$\hat{\sigma}(q\bar{q} \to W_\mu^{(1,1)3}) = \frac{\pi^2\alpha (\xi_q^W C^G)^2}{12\sin^2\theta_w M_{W^{(1,1)}}} \delta(\sqrt{\hat{s}} - M_{W^{(1,1)}}), \tag{4.9}$$

$$\hat{\sigma}(q\bar{q} \to B_\mu^{(1,1)}) = \frac{\pi^2\alpha (C^G)^2}{12\cos^2\theta_w M_{B^{(1,1)}}} (a_{q_L} + a_{q_R}) \times \delta(\sqrt{\hat{s}} - M_{B^{(1,1)}}). \tag{4.10}$$

The total production cross section at the Tevatron are given by

$$\sigma(p\bar{p} \to W_\mu^{(1,1)3}) = \frac{\pi^2\alpha (C^G)^2}{6\sin^2\theta_w s} \sum_q (\xi_q^W)^2 t_q(M^2_{W_\mu^{(1,1)}}/s),$$
$$\sigma(p\bar{p} \to B_\mu^{(1,1)}) = \frac{\pi^2\alpha (C^G)^2}{6\cos^2\theta_w s} \sum_q (a_{q_L} + a_{q_R}) t_q(M^2_{B_\mu^{(1,1)}}/s), \tag{4.11}$$

and are shown in Fig. 3. Note that the $B_\mu^{(1,1)}$ production is suppressed compared to $W_\mu^{(1,1)3}$ production by a $\tan^2\theta_w$ factor, but it is also enhanced by the larger values of the ξ parameters, such that the curves representing the two cross sections are very close to each other.

B. Peaks in the invariant mass distributions

Once produced at the Tevatron, the $G_\mu^{(1,1)}$, $W_\mu^{(1,1)3}$, and $B_\mu^{(1,1)}$ would decay with the branching fractions given in Tables III and IV. These vector (1,1) modes are leptophobic (only $B_\mu^{(1,1)}$ has a potentially interesting branching fractions of about 1% into each lepton pair), but have rather large branching fractions into $t\bar{t}$ pairs, either directly or via cascade decays as explained at the end of Sec. III E.

Altogether there are six resonances that can be produced in the $t\bar{t}$ invariant mass distribution: the vector and spinless (1,1) modes of the gluon and of the two electroweak gauge bosons. However, the decay $G_\mu^{(1,1)} \to t\bar{t}$ has a negligible branching fraction. Therefore, we will concentrate on the $t\bar{t}$ peaks at the masses of $G_H^{(1,1)}$, $W_\mu^{(1,1)3}$, $B_\mu^{(1,1)}$, $W_H^{(1,1)3}$, and $B_H^{(1,1)}$. These are given by $1.10M_{1,1}$, $1.08M_{1,1}$, $0.98M_{1,1}$, $0.95M_{1,1}$, and $0.86M_{1,1}$, where $M_{1,1} = \sqrt{2}/R$.

The spinless (1,1) gluon, $G_H^{(1,1)}$, is produced only in cascade decays of the vector (1,1) gluon, as shown in Fig. 4, the electroweak spinless adjoints are produced in the cascade decays of both $W_\mu^{(1,1)3}$ (see Fig. 5) and $G_\mu^{(1,1)}$, while the electroweak vector modes are produced both in cascade decays and directly, as shown in Fig. 5. The cross sections for producing $t\bar{t}$ pairs with an invariant mass corresponding to the five resonances are given by

$$\begin{aligned}
\sigma_{t\bar{t}}(G_H^{(1,1)}) &= \sigma(G_\mu) b_G(G_H), \\
\sigma_{t\bar{t}}(W_\mu^{(1,1)3}) &= [\sigma(G_\mu) b_G(W_\mu^3) + \sigma(W_\mu^3)] b_W(t\bar{t}), \\
\sigma_{t\bar{t}}(B_\mu^{(1,1)}) &= [\sigma(G_\mu) b_G(B_\mu) + \sigma(W_\mu^3) b_W(B_\mu) \\
&\quad + \sigma(B_\mu)] b_B(t\bar{t}), \\
\sigma_{t\bar{t}}(W_H^{(1,1)3}) &= \sigma(G_\mu) b_G(W_H^3) + \sigma(W_\mu^3) b_W(W_H^3), \\
\sigma_{t\bar{t}}(B_H^{(1,1)}) &= \sigma(G_\mu) b_G(B_H) + \sigma(W_\mu^3) b_W(B_H),
\end{aligned} \tag{4.12}$$

where we introduced the shorthand notations

$$\sigma(V_\mu) \equiv \sigma(p\bar{p} \to V_\mu^{(1,1)} X), \tag{4.13}$$

for the production cross sections shown in Fig. 3, and

$$\begin{aligned}
b_G(V) &\equiv \mathrm{Br}(G_\mu^{(1,1)} \to V^{(1,1)} + \text{jets}), \\
b_W(V) &\equiv \mathrm{Br}(W_\mu^{(1,1)3} \to V^{(1,1)} + \text{leptons}), \\
b_V(t\bar{t}) &\equiv \mathrm{Br}(V_\mu^{(1,1)} \to t\bar{t}).
\end{aligned} \tag{4.14}$$

for the branching fractions given in Tables III and IV. In Eq. (4.12) we have used branching fractions of 100% for

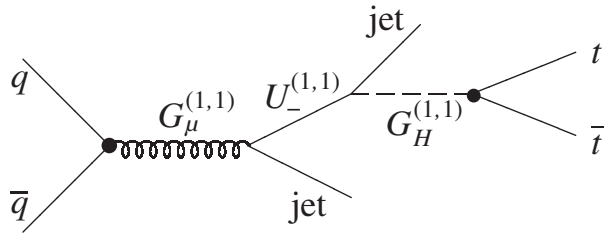

FIG. 4. Production of the vector (1,1) gluon followed by a cascade decay. The • stands for a KK-number-violating coupling. Other diagrams having the same topology exist: the $U_-^{(1,1)}$ quark KK mode may be replaced by $D_-^{(1,1)}$, $Q_+^{(1,1)}$, or the corresponding antiquarks; in addition the spinless gluon $G_H^{(1,1)}$ may be replaced by $B_\mu^{(1,1)}$ or $B_H^{(1,1)}$, and in the case where the quark KK mode is an $SU(2)_W$ doublet, by $W_\mu^{(1,1)3}$ or $W_H^{(1,1)3}$.

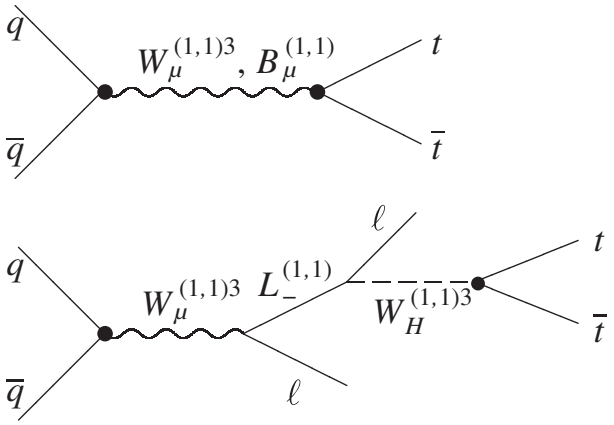

FIG. 5. Production of W_μ^3 and B_μ (1,1) modes, followed by representative decays.

electrically-neutral spinless adjoints into $t\bar{t}$, which is a reasonably good approximation.

Additional contributions to the $t\bar{t}$ peaks at the $B_\mu^{(1,1)}$, $W_H^{(1,1)3}$ and $B_H^{(1,1)}$ masses come from s-channel production of $W_\mu^{(1,1)\pm}$ followed by cascade decays similar to the one in Fig. 5. However, the relevant branching fractions for $W_\mu^{(1,1)\pm}$ are at most a few percent, and for simplicity we ignore them. We have also neglected contributions to Eq. (4.12) coming from the cascade decays of a (1,1) KK gluon through a $W_\mu^{(1,1)}$ into $B_\mu^{(1,1)}$, $W_H^{(1,1)3}$ or $B_H^{(1,1)}$, because these are suppressed by an additional branching ratio.

The five resonances described above are very narrow, but cannot be separately resolved at hadron collider experiments. At CDF and D0, the $t\bar{t}$ pair mass resolution is expected to be around 10%, so one could hope for at most three distinct peaks. The heaviest one corresponds to the $G_H^{(1,1)}$ and $W_\mu^{(1,1)3}$ resonances which have masses 2% apart, with an average of $1.09M_{1,1}$. Then, there is a peak at $0.97M_{1,1}$, composed of $W_H^{(1,1)}$ and $B_\mu^{(1,1)}$, whose masses separated by 3% cannot be resolved experimentally. The third peak, due to $B_H^{(1,1)}$, is at $0.86M_{1,1}$.

In Fig. 6 we plot the cross sections for $t\bar{t}$ pairs coming from the three mass peaks. The current preliminary limits at the 95% confidence level from D0 [20] and CDF [21] on the production cross section of a narrow $t\bar{t}$ resonance, based on 0.37 fb^{-1} and 0.32 fb^{-1} of Run II data, respectively, are around 1 pb for $M(t\bar{t})$ above 600 GeV or so, and a few times larger than that for $M(t\bar{t})$ in the 350–550 GeV range due to some excess events. The $G_H^{(1,1)} + W_\mu^{(1,1)3}$ and $W_H^{(1,1)3} + B_\mu^{(1,1)}$ mass peaks have cross sections not far below these limits, but at the moment $1/R$ is not constrained by s-channel production of (1,1) modes.

Nevertheless, the much larger integrated luminosity expected until the end of Run II will make it possible to probe an interesting range of values for the compactification scale. In order to estimate the ultimate reach of the Tevatron, we plot in Fig. 7 the sum of the cross sections

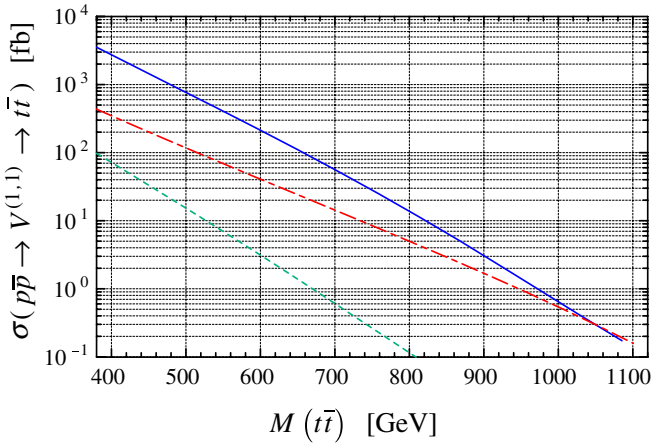

FIG. 6 (color online). Cross section for the production of $t\bar{t}$ pairs at the Tevatron from the three distinct mass peaks: $G_H^{(1,1)} + W_\mu^{(1,1)3}$ (top, solid line), $W_H^{(1,1)3} + B_\mu^{(1,1)}$ (middle line) and $B_H^{(1,1)}$ (bottom line).

into $t\bar{t}$ pairs from all peaks versus the uncorrected mass of the (1,1) KK level, i.e., $M_{1,1} = \sqrt{2}/R$. One should keep in mind that for any given value of $1/R$ the separation between consecutive mass peaks is slightly above 10%. For instance, for $1/R = 500$ GeV, the peaks are at 770 GeV, 680 GeV, and 610 GeV. For this value of the compactification scale, the total cross section for $t\bar{t}$ pairs from (1,1) resonances is approximately 40 fb. The branching fraction for $t\bar{t}$ into the lepton plus jets final state used in [20,21] is 29%, while the product of acceptance times efficiency is expected to be in the 15%–20% range. Therefore, approximately 5% of the $t\bar{t}$ pairs can be selected, so that an integrated luminosity of 5 fb^{-1} will result in a total of about 10 reconstructed $t\bar{t}$ events from the sum of all (1,1) resonances, for $1/R = 500$ GeV.

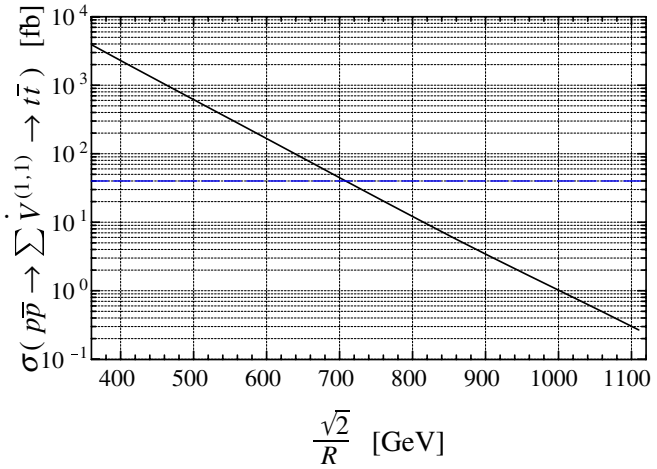

FIG. 7 (color online). Cross section for the production of $t\bar{t}$ pairs at the Tevatron from the sum of all mass peaks at KK level (1,1), as a function of $M_{1,1} = \sqrt{2}/R$. The dashed horizontal line marks 10 selected events with 5 fb^{-1}, assuming that 5% of the $t\bar{t}$ pairs are selected.

Although the background is small, due especially to standard model $t\bar{t}$ and $W + 4j$ productions [20], it is not negligible at large luminosity for $M(t\bar{t})$ below 800 GeV or so, and therefore the ultimate Tevatron reach is likely to be below $1/R = 500$ GeV.

An estimate of the future sensitivity to $t\bar{t}$ resonances [22] shows that with 4 fb^{-1} the production cross section will be down to 1.3 pb for a mass of 450 GeV, and 0.7 pb for a mass of 550 GeV. Comparing these numbers with the cross section for the $G_H^{(1,1)} + W_\mu^{(1,1)3}$ mass peak given in Fig. 6, we find that there will be sensitivity to a peak of mass up to 480 GeV. Given that Run II may deliver more than 4 fb^{-1}, and that there are additional $t\bar{t}$ events from the nearby $W_H^{(1,1)3} + B_\mu^{(1,1)}$ mass peak, it is likely that the ultimate Tevatron sensitivity will be for a $G_H^{(1,1)} + W_\mu^{(1,1)3}$ mass peak above 500 GeV, corresponding to a limit of 320 GeV on $1/R$.

A cautionary comment needs to be made: the preliminary D0 and CDF limits mentioned above have been derived based on the assumption that there is a single $t\bar{t}$ resonance having a width equal to 1.2% of its mass [20,21]. In the model with two universal extra dimensions discussed here, there are several resonances arising from both direct production and cascade decays, and therefore one would need to set limits based on these facts. However, the extra jets and leptons that are produced in the cascade decays are relatively soft due to the approximate mass degeneracy of the (1,1) modes, and are not likely to change dramatically the limits. The individual resonances are very narrow (with widths of at most 0.1% of their mass for the electroweak KK bosons, and of the order of 1% for $G_H^{(1,1)}$), but the main ones come in pairs, with separations of 2–3% within the pairs. Given the expected resolution of 10%, such a pair of resonances looks like a single resonance, similar to the one used to set the CDF and D0 limits. The presence of two pairs (the top two curves in Fig. 6) with comparable cross sections, which may partially overlap, is likely to have a stronger impact on the limits. Overall though this is not a concern at the level of accuracy employed here.

So far, we have assumed in this section that the KK mass splittings and KK-number-violating couplings are given by the one-loop effects discussed in Sec. II. We reiterate that there are uncertainties in the mass splittings and couplings to zero modes of the (1,1) modes due to higher loops involving the $SU(3)_C$ interactions (see Sec. II B). These could have several effects. For example, the mass of $G_H^{(1,1)}$ could be further apart from the mass of $W_\mu^{(1,1)3}$. However, it turns out that the majority of events in the $G_H^{(1,1)} + W_\mu^{(1,1)3}$ mass peak are due to $G_H^{(1,1)}$, so that the uncertainty in the mass of $G_H^{(1,1)}$ does not result into a changed sensitivity to the highest peak, but rather into an uncertainty on the limit on $1/R$. A more drastic effect of the higher loops would be to invert the mass hierarchy between the (1,1) quarks and

$G_H^{(1,1)}$. In that case the $t\bar{t}$ peak at the $G_H^{(1,1)}$ mass would be highly suppressed, but a large fraction of the $G_\mu^{(1,1)}$ cascade decays would result in $t\bar{t}$ events at the mass peaks due to the (1,1) electroweak bosons (see Sec. III D).

If the qualitative mass hierarchy of (1,1) modes is the one given by the one-loop results, then shifts in two parameters from higher loops could have a substantial impact on the production cross section of the $t\bar{t}$ resonances. First, the mass splitting between $G_\mu^{(1,1)}$ and $G_H^{(1,1)}$ could be different. If it is larger (smaller), then the cross section for a given $G_H^{(1,1)}$ mass decreases (increases), as it is harder (easier) to produce the $G_\mu^{(1,1)}$ boson, which is the main source of $G_H^{(1,1)}$ production, via cascade decays.

Second, the average coupling of $G_\mu^{(1,1)}$ to quark zero-modes, ξ_q^G [see Eqs. (2.25) and (2.29)], may also be different than the one-loop result. Assuming that the change in ξ_q^G is at most a factor of 2, the cross section for the $t\bar{t}$ signal due to $G_H^{(1,1)}$ decays (approximately given by the top curve in Fig. 6) could still increase by a factor of 4, because the cross section is proportional to $(\xi_q^G)^2$, as shown in Eq. (4.3). In that case the CDF and D0 sensitivity from Ref. [22] with 4 fb^{-1} would increase to a $G_H^{(1,1)}$ mass of about 700 GeV. Notice also that a large decrease in ξ_q^G would not necessarily dilute completely the Tevatron reach, since the $W_\mu^{(1,1)}$ and $B_\mu^{(1,1)}$ production cross sections depend on parameters other than ξ_q^G (those parameters, ξ_q^W and ξ_q^B, are affected by higher loops that change the wave function renormalization of the quarks, but their shifts may be different than for ξ_q^G). Based on these considerations, we conclude that the ultimate Tevatron sensitivity to $t\bar{t}$ mass peaks from the 6D standard model may be as high as in the 0.5–0.7 TeV range (corresponding to $1/R$ as high as 320–450 GeV), depending on the values of parameters controlled by the $SU(3)_C$ interactions of the KK modes.

For low enough $1/R$ one may hope for a discovery of $t\bar{t}$ resonances at the Tevatron. In that case one should find ways of discriminating the models with two universal extra dimensions against other models that predict $t\bar{t}$ resonances, such as Topcolor [23] or certain technicolor models [24]. Fortunately, the extra jets and leptons from cascade decays may provide useful checks for confirming that the resonances are due to (1,1) modes. The jets come from decays of the colored (1,1) states as shown in Fig. 4, and may carry an energy of up to 10–15% of the mass of the decaying particle. The leptons come from cascade decays of $W_\mu^{(1,1)3}$ (see Fig. 5), with rather small but still relevant branching fractions given in Table III. Measurements of angular distributions may further discriminate among various models.

In addition to the decays into $t\bar{t}$ pairs from the above mentioned resonances, there will be decays of $W_\mu^{(1,1)}$, $B_\mu^{(1,1)}$, and (to a lesser extent, see Table IV) of $G_\mu^{(1,1)}$ into a pair of jets. From Table III, we see that $\mathrm{Br}(W_\mu^{(1,1)3} \to \text{dijets}) = 64\%$ and $\mathrm{Br}(B_\mu^{(1,1)} \to \text{dijets}) = 71\%$, where we included b jets. Figure 3 shows that dijet resonances at the $W_\mu^{(1,1)3}$ and $B_\mu^{(1,1)}$ masses are produced with cross sections of tens of femtobarns, for $1/R \simeq 500$ GeV. The search for dijet resonances is a great challenge due to large backgrounds [25,26], but an observation at invariant masses consistent with the $t\bar{t}$ peaks would provide a further confirmation of the models with universal extra dimensions.

Here we have concentrated on single production of (1,1) modes. The pair production of (1,0) modes is also interesting, and needs to be analyzed in detail. In the case of one universal extra dimension, a search in the leptons plus missing-energy channel in Run I is already setting a limit of $1/R > 280$ GeV at the 95% confidence level [27]. In order to set limits on two universal extra dimensions based on pair production of (1,0) modes, one needs to use the KK-number preserving interactions derived in Ref. [11] and compute the relevant cross sections and branching fractions. Compared to the case of one universal extra dimension, the presence of spinless adjoints could substantially change both the cross sections for pair production [28] and the branching fractions [5]. We leave this important study for future work.

V. PROSPECTS FOR THE LHC

By contrast to the Tevatron, where the dominant contribution to the production of (1,1) modes comes from $q\bar{q}$ annihilation, at the LHC there will be competing contributions from parton-level processes involving gluons in the initial state. The KK-number-violating couplings of gluons arise from higher-dimensional operators generated at the one-loop level. Although these couplings are not enhanced by a logarithmic factor, as the $q\bar{q}$ couplings to vector modes (see section II D), the presence of the gluon in the initial state may compensate this effect due to a larger PDF at moderate energies. The main processes are s-channel production due to dimension-6 operators of the $G_\mu^{(1,1)}$ and $B_\mu^{(1,1)}$ vector modes through gluon fusion, and of the (1,1) quark modes through quark-gluon fusion. It is beyond the scope of this article to compute the coefficients of these operators which arise from finite one-loop contributions. In order to have an order of magnitude estimate of (1,1)-mode production at the LHC we compute the $q\bar{q}$ annihilation processes which have logarithmic enhancements of the couplings but smaller PDF's for $\bar{q}$.

The production cross sections at the LHC for $G_\mu^{(1,1)}$, $W_\mu^{(1,1)3}$, and $B_\mu^{(1,1)}$ due to $q\bar{q}$ annihilation are given by the right-hand sides of Eqs. (4.3) and (4.11) with $t_q(z)$ replaced by

$$\int_z^1 \frac{dx}{x}[q(x)\bar{q}(z/x) + \bar{q}(x)q(z/x)], \tag{5.1}$$

to leading order in α_s. In Fig. 8 we plot these three cross sections, using the CTEQ6 PDF's at leading order with a K

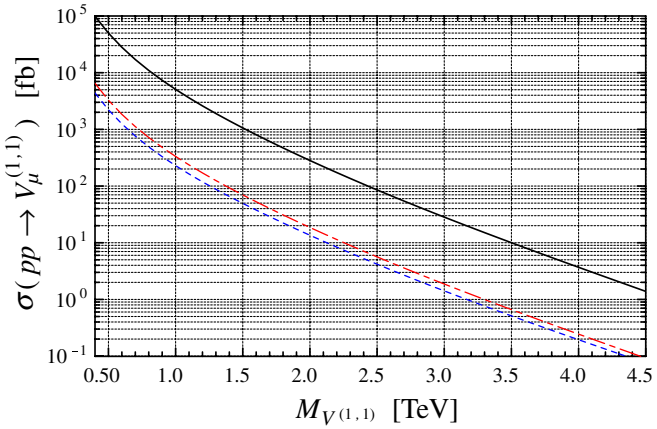

FIG. 8 (color online). Production cross sections for (1,1) vector modes in the s channel at the LHC due to $q\bar{q}$ annihilation. The solid, dashed and dotted (lowest) lines represent the $G_\mu^{(1,1)}$, $W_\mu^{(1,1)3}$ and $B_\mu^{(1,1)}$ production cross sections, respectively.

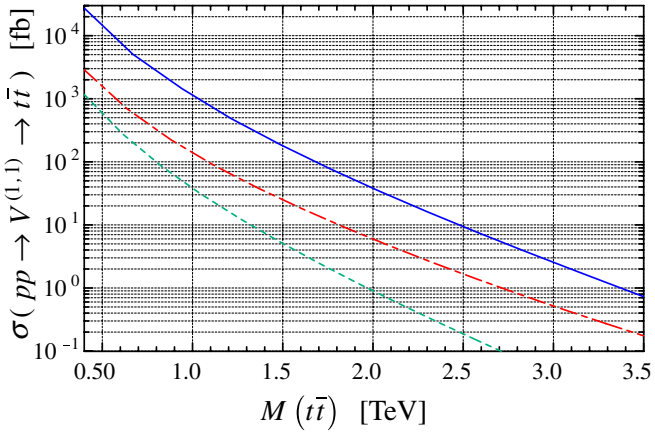

FIG. 9 (color online). Cross section for the production of $t\bar{t}$ pairs at the LHC from the $G_H^{(1,1)} + W_\mu^{(1,1)3}$ (top, solid line), $W_H^{(1,1)3} + B_\mu^{(1,1)}$ (middle line), and $B_H^{(1,1)}$ (bottom line) peaks.

factor of 1.3. In the case of $G_\mu^{(1,1)}$, and $B_\mu^{(1,1)}$, these are underestimates of the total production cross sections because the additional contributions to the production cross sections from gluon fusion mentioned above are not included. For $W_\mu^{(1,1)3}$ production, the $SU(2)_W$ gauge symmetry does not allow gluon fusion via dimension-6 operators, and therefore the only relevant parton-level process is $q\bar{q} \to W_\mu^{(1,1)3}$. One should keep in mind though that additional $W_\mu^{(1,1)3}$ particles are produced from the cascade decays of $G_\mu^{(1,1)}$, as explained in Sec. III E.

In order to translate these high rates at the LHC into a mass reach it is necessary to study carefully the backgrounds, which are huge for values of $1/R$ in the few hundred GeV, where the Tevatron has a significant discovery potential. For larger values of the compactification scale, the backgrounds should be manageable for the $t\bar{t}$ signal. Moreover, for large $1/R$ the decay of $G_\mu^{(1,1)}$ to a top quark and its (1,1) mode opens up (see Sec. III E), leading to additional interesting signals involving t and b quarks. Thus, the LHC will complement the searches at the Tevatron discussed in Sec. IV, by probing larger values of $1/R$.

In Fig. 9 we plot the cross sections for $t\bar{t}$ pairs coming from the $G_H^{(1,1)} + W_\mu^{(1,1)3}$, $W_H^{(1,1)3} + B_\mu^{(1,1)}$, and $B_H^{(1,1)}$ mass peaks, including only the $q\bar{q}$ initial states. Comparing these cross sections to the discovery potential of the ATLAS detector for a narrow resonance decaying to $t\bar{t}$, given in [29,30], we estimate that the production cross sections for (1,1) modes are large enough to allow discovery of narrow $t\bar{t}$ resonances of at least 1 TeV with an integrated luminosity of 30 fb^{-1}. The reach can be further increased by using the extra leptons produced in the cascade decays of the $W_\mu^{(1,1)3}$ and $W_\mu^{(1,1)\pm}$ modes, as shown in Fig. 5.

If a discovery is made, further measurements may be performed: angular distributions, threshold effects in cascade decays, lepton pairs from $B_\mu^{(1,1)}$ decays (the branching fraction is 1% for each of the e^+e^- and $\mu^+\mu^-$ pairs). A thorough study of the capabilities of the LHC, both in the hadronic and leptonic channels is needed. Particularly exciting would be to identify the spinless adjoints, since the presence of these states is a distinctive feature of the 6D scenario.

The most convincing test of the existence of two universal extra dimensions would be the observation of series of resonances clustered around the masses of the (j, k) levels with $j + k$ even. Relative to the first even level, of mass $M_{1,1} = \sqrt{2}/R$, the next four even levels have masses $M_{2,0} = \sqrt{2}M_{1,1}$, $M_{2,2} = 2M_{1,1}$, $M_{3,1} = \sqrt{5}M_{1,1}$, $M_{4,0} = 2\sqrt{2}M_{1,1}$. Within each of these levels, the relative mass splittings are roughly the same as for the (1,1) level (see Fig. 1). However, the branching fractions into zero-mode fermions are smaller than for the corresponding (1,1) mode because the higher-level KK modes may also decay into lower level ones.

VI. CONCLUSIONS

The 6D standard model compactified on the chiral square [10,11] is a well motivated theory, given that it predicts a long proton lifetime [31], it restricts the number of fermion generations to a multiple of three [8], and it accommodates nicely the observed pattern of neutrino oscillations [9]. We have computed here the spectrum of KK modes, which is split due to localized operators induced by one-loop effects (see Sec. II). In particular, we have shown that the lightest KK particle in this model is the hypercharge spinless adjoint $B_H^{(1,0)}$, whose mass is roughly 15% below the compactification scale $1/R$ which sets the tree-level mass of the (1,0) KK modes. This appears to be a promising dark matter candidate, but in order to find the range of values for $1/R$ consistent with the dark matter abundance one would need to determine the relic density

along the lines of the detailed computations performed in the case of one universal extra dimension [32,33].

We have also computed the KK-number-violating interactions due to loop-induced localized operators which, although suppressed compared to the tree-level interactions presented in Ref. [11], have important phenomenological consequences. In this way we have laid the groundwork for studies of the phenomenology of two universal extra dimensions.

After completing this general study of the KK couplings and masses, we have focused on the (1,1) modes, which are even under KK-parity, and therefore may be produced in the s channel at colliders. The (1,1) modes are the lightest KK modes of this type, with a tree-level mass of only $\sqrt{2}/R$. This low mass for an even KK level, and the presence of spinless adjoints changes significantly the phenomenology compared to the case of level-2 modes from one universal extra dimension discussed in Refs. [5,7].

In Sec. III we have computed the branching fractions of the (1,1) KK modes. As in the case of one universal extra dimension, the even vector modes are leptophobic because the loop-induced couplings to zero-mode leptons are generated by the $SU(2)_W \times U(1)_Y$ interactions, while the loop-induced couplings to zero-mode quarks are generated by the $SU(3)_C$ interactions. Only the hypercharge (1,1) mode has a non-negligible branching fractions into lepton pairs: 1% for each of e^+e^- and $\mu^+\mu^-$. An interesting result of our computation is that the branching fractions to $t\bar{t}$ pairs are enhanced, especially because the strength of the (1,1) couplings to the top quark is increased by one-loop corrections involving the Yukawa interaction to the Higgs fields. Even more strikingly, the spinless adjoints decay most of the time into $t\bar{t}$ pairs, because their couplings to zero-mode fermions are proportional to the fermion mass. Putting together the direct decays and cascade decays of vector (1,1) modes, we have found large branching fractions for final states involving $t\bar{t}$ resonances: 72%, 21%, and 26% for $G_\mu^{(1,1)}$, $W_\mu^{(1,1)3}$, and $B_\mu^{(1,1)}$, respectively, for $1/R \sim 500$ GeV.

Although leptophobic bosons are usually hard to observe at hadron colliders, due to large backgrounds, the sizable branching fractions into $t\bar{t}$ offer promising prospects for searches at the Tevatron and the LHC. We have shown that the Tevatron is likely to set useful limits on $1/R$, through s-channel production of the (1,1) gluon, $B_\mu^{(1,1)}$ and $W_\mu^{(1,1)3}$, and their subsequent cascade or direct decays to a pair of top quarks (see Sec. IV B). Altogether there are five narrow resonances to be observed in the invariant $t\bar{t}$ mass distribution, but they form at most three mass peaks once we take into account a realistic $t\bar{t}$ pair mass resolution. With 4 fb^{-1}, the D0 and CDF experiments may discover resonances in the $t\bar{t}$ channel, or else will likely set a lower limit on $t\bar{t}$ mass peaks in the 500–700 GeV range, corresponding to a lower limit on $1/R$ in the 320–450 GeV range.

If a discovery of one or more $t\bar{t}$ resonances is made at the Tevatron, or for larger $1/R$ at the LHC, there are various other measurements that can differentiate the 6D standard model from other theories, such as Topcolor [23], that predict similar resonances. Particularly useful would be measurements of the extra jets and leptons from cascade decays, angular distributions in the decays of spinless adjoints, the dijet invariant mass distribution that may reveal resonances with the same mass as in the $t\bar{t}$ channel, and signals involving missing transverse energy from pair production of (1,0) modes.

Despite the troublesome backgrounds at the LHC, the large rates for producing $t\bar{t}$ resonances at high invariant mass, in the TeV range, would allow accurate measurements. For a precise assessment of the LHC reach in $1/R$, more detailed studies are needed. Particularly exciting would be the discovery of resonances associated with several KK levels. The masses of consecutive even levels have ratios given by a peculiar factor of $\sqrt{2}$ for the first three even levels, so that the observation of clusters of resonances fitting this pattern would signal the existence of two universal extra dimensions.

ACKNOWLEDGMENTS

We are grateful to Robert Harris, Jacobo Konigsberg, and Greg Landsberg for illuminating explanations regarding the capabilities of CMS, CDF, and D0. We would like to thank Elizabeth Simmons and Hitoshi Murayama for comments regarding KK-mode production, and Frank Petriello for a couple of useful observations. G. B. acknowledges the support of the State of São Paulo Research Foundation (FAPESP), and the Brazilian National Counsel for Technological and Scientific Development (CNPq). The work of B. D. was supported by DOE under Contract No. DE-FG02-92ER-40704. E. P. was supported by DOE under Contract No. DE-FG02-92ER-40699.

[1] K. R. Dienes, E. Dudas, and T. Gherghetta, Nucl. Phys. **B537**, 47 (1999).

[2] K. m. Cheung and G. Landsberg, Phys. Rev. D **65**, 076003 (2002); T. G. Rizzo and J. D. Wells, Phys. Rev. D **61**, 016007 (2000).

[3] For a more optimistic assessment, see E. Accomando, I.

Antoniadis, and K. Benakli, Nucl. Phys. **B579**, 3 (2000).
[4] T. Appelquist, H. C. Cheng, and B. A. Dobrescu, Phys. Rev. D **64**, 035002 (2001).
[5] H. C. Cheng, K. T. Matchev, and M. Schmaltz, Phys. Rev. D **66**, 056006 (2002).
[6] H. C. Cheng, K. T. Matchev, and M. Schmaltz, Phys. Rev. D **66**, 036005 (2002).
[7] A. Datta, K. Kong, and K. T. Matchev, Phys. Rev. D **72**, 096006 (2005); **72**, 119901E (2005).
[8] B. A. Dobrescu and E. Poppitz, Phys. Rev. Lett. **87**, 031801 (2001).
[9] T. Appelquist, B. A. Dobrescu, E. Pontón, and H. U. Yee, Phys. Rev. D **65**, 105019 (2002).
[10] B. A. Dobrescu and E. Pontón, J. High Energy Phys. 03 (2004) 071.
[11] G. Burdman, B. A. Dobrescu, and E. Ponton, J. High Energy Phys. 02 (2006) 033.
[12] E. Pontón and L. Wang, hep-ph/0512304.
[13] H. Georgi, A. K. Grant, and G. Hailu, Phys. Lett. B **506**, 207 (2001).
[14] G. Servant and T. M. P. Tait, Nucl. Phys. **B650**, 391 (2003); H. C. Cheng, J. L. Feng, and K. T. Matchev, Phys. Rev. Lett. **89**, 211301 (2002).
[15] Z. Chacko, M. A. Luty, and E. Pontón, J. High Energy Phys. 07 (2000) 036.
[16] T. Appelquist and H. U. Yee, Phys. Rev. D **67**, 055002 (2003).
[17] K. S. Babu, C. F. Kolda, and J. March-Russell, Phys. Rev. D **54**, 4635 (1996).
[18] J. Pumplin, D. R. Stump, J. Huston, H. L. Lai, P. Nadolsky, and W. K. Tung, J. High Energy Phys. 07 (2002) 012.
[19] M. Carena, A. Daleo, B. A. Dobrescu, and T. M. P. Tait, Phys. Rev. D **70**, 093009 (2004).
[20] D0 Collaboration Report No. 4880-CONF, 2005; www-d0.fnal.gov/Run2Physics/WWW/results/top.htm.
[21] CDF Collaboration, "Search for resonant $t\bar{t}$ production in $p\bar{p}$ collisions at $\sqrt{s} = 1.96$ TeV," CDF Report No. 7971, 2005; www-cdf.fnal.gov/physics/new/top/top.html.
[22] R. Rossin, "Measurements of top quark pair production cross section and search for resonances at the Tevatron," International Workshop, January 12, 2006 (University of Coimbra, Portugal, to be published).
[23] C. T. Hill, Phys. Lett. B **266**, 419 (1991); C. T. Hill and S. J. Parke, Phys. Rev. D **49**, 4454 (1994); R. M. Harris, *Discovery Mass Reach for Topgluons Decaying to t Anti-T at the Tevatron*, eConf C960625, NEW166 (1996); R. M. Harris, C. T. Hill, and S. J. Parke, hep-ph/9911288.
[24] K. D. Lane and E. Eichten, Phys. Lett. B **222**, 274 (1989).
[25] V. M. Abazov *et al.* (D0 Collaboration), Phys. Rev. D **69**, 111101 (2004); F. Abe *et al.* (CDF Collaboration), Phys. Rev. D **55**, R5263 (1997).
[26] E. H. Simmons, Phys. Rev. D **55**, 1678 (1997).
[27] C. Lin, FERMILAB Report No. FERMILAB-PUB-05-572-E.
[28] C. Macesanu, C. D. McMullen, and S. Nandi, Phys. Rev. D **66**, 015009 (2002); T. G. Rizzo, Phys. Rev. D **64**, 095010 (2001); J. M. Smillie and B. R. Webber, J. High Energy Phys. 10 (2005) 069.
[29] ATLAS, Technical design Report No. CERN-LHCC-99-15, Vol. 2, Chap. 18.
[30] M. Beneke *et al.*, hep-ph/0003033.
[31] T. Appelquist, B. A. Dobrescu, E. Pontón, and H. U. Yee, Phys. Rev. Lett. **87**, 181802 (2001).
[32] K. Kong and K. T. Matchev, J. High Energy Phys. 01 (2006) 038; F. Burnell and G. D. Kribs, Phys. Rev. D **73**, 015001 (2006).
[33] M. Kakizaki, S. Matsumoto, Y. Sato, and M. Senami, Nucl. Phys. **B735**, 84 (2006).